

THE INFLUENCE OF HALOGENATED SPECIES ON OZONE AND PRECURSORS IN THE LOWER TROPOSPHERE.

Asgeir Sorteberg* and Øystein Hov†
The Norwegian Meteorological Institute

Abstract

The possible role of gas phase chlorine and bromine compounds influence on ozone and precursors in the mid latitude tropospheric marine environment is investigated. The interaction between gas phase chlorine and bromine chemistry is discussed with emphasis on non-linearities in the ozone depletion potential when both compounds are present.

An extensive chlorine and bromine chemistry was implemented into an Eulerian 3-D model and run in a case study with clean air with small amounts of *NMHC* and *NO_x*. The emissions of halogens were prescribed to correspond to measured concentrations. Even though *BrO* and *ClO* had average concentrations below 0.5 and 3 ppt, respectively. The inclusion of the halogens oxidized 10-15% more of the *NMHCs* compared to a run without halogens. This increased the daytime peak of *RO₂* with 15-30% and increased the *HCHO* concentration on average 10-20%. The halogens were shown to have little effect on ozone (1-4% reduction) due to the low amounts of bromine.

The competition between diffusion, advection, convection and chemistry in changing the concentrations was investigated. Even though the emission were held constant, differences in vertical transport within the model area altered the total bromine and chlorine concentration at the surface by almost one order of magnitude, demonstrating the importance of taking into account boundary layer meteorological parameters in the interpretation of observed concentrations.

1 Introduction

Episodic boundary layer ozone depletion events in the Arctic in spring (Barrie et al., 1988; Bottenheim, 1990; Solberg et al., 1996) put focus on the potential importance of halogens in

*Corresponding author address: Asgeir Sorteberg, The Norwegian Meteorological Institute, P.O. Box 43, Blindern N-0313 Oslo, Norway. Email: a.sorteberg@dnmi.no

†Norwegian Institute for Air Research (NILU)

tropospheric chemistry. Measurements of alkanes, alkenes and alkynes (Jobson et al., 1994; Solberg et al., 1996; Ramacher et al., 1997), formaldehyde measurements (de Serves, 1994), NO_x measurements (Beine et al., 1997) and the possible influence of halogens as a sink of *DMS* (Toumi, 1994) point to the large oxidation capacity of chlorine and bromine compounds.

Few calculations have been made of the role of halogens in the atmospheric boundary layer at mid latitudes (Sander and Crutzen, 1996; Vogt et al., 1996). In this paper we address how gas phase halogen chemistry affect the production and loss of ozone and precursors. An extensive gas phase reaction scheme of bromine and chlorine compounds has been added to a simplified hydrocarbon chemistry in order to investigate the possible role of reactive halogen species for 'background' concentrations of the halogens. The background levels are based on measurement at mid latitude in the HALOTROP project (Platt et al., 1998), and on previous Arctic measurements (Hausmann and Platt, 1994; Tuckermann et al., 1997). These measurements have often been below detection limits, making it difficult to quantify a background level.

The halogen chemistry was incorporated into a 3D numerical model of troposphere chemistry and transport, coupled to a meteorological limited area model, to investigate the competition between chemical and physical processes in the determining the fate of the halogen radicals under a typical clean air event.

Due to lack of knowledge of the emissions of halogens the emissions were prescribed to correspond to the measured concentrations. The lack of emission data has made it necessary to focus on concentration ratios and on the relative contribution within the group of halogen compounds to reduce the sensitivity of the results to absolute emission rates.

2 Discussion of model chemistry

The gas phase chemistry is listed in Table 3 and consists of an extensive bromine and chlorine chemistry and a simplified hydrocarbon chemistry with lumped species. Ethane represents a typical alkane, ethene a typical alkene and ethyne a typical alkyne. Their concentrations are therefore not directly comparable to observed values, but represent lumped values. Halogen compounds taken into account are *Br*, *Br₂*, *BrO*, *HOBr*, *BrONO₂*, *HBr*, *BrCl*, *Cl*, *Cl₂*, *ClO*, *Cl₂O₂*, *HOCl*, *ClONO₂* and *HCl*. Special emphasis is made on bromine - chlorine interactions in order to investigate the partitioning between the different halogen compounds, when no heterogenous or wet phase reactions are involved. Reaction rates have been taken from recent literature. However, products of *Br* reactions with hydrocarbons are not well known and assumed to be in the form of *HBr*. Decomposition of *OCIO* to $O(^3P) + ClO$ and XOO ($X = Br$ and Cl) to $X + O_2$ is assumed to be fast. In Figure 1 the halogen containing reactions accounted for in the gas phase are shown.

2.1 Interaction of Bromine and chlorine gas phase chemistries.

Ozone destruction by bromine mainly takes place in reactions with bromine radicals where *Br* atoms are oxidized by ozone to *BrO* and where most of the *BrO* will photolyse back to *Br*

and $O(^3P)$ with no net effect on ozone,



However, in several chain reactions BrO is converted to Br without producing oxygen atoms and there is a net ozone loss.

A Br/BrO catalytic cycle was suggested by Barrie et al., 1988:

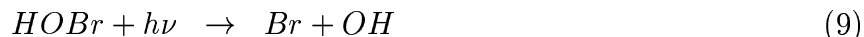
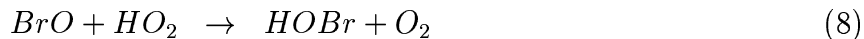


where the BrO self reaction is the rate limiting step. A branch of the BrO self reaction produces Br_2 instead of Br with a rate which is about 15 times slower at 288 K.



Figure 1: Scheme of bromine and chlorine reactions in the gas phase accounted for in model.

In the presence of peroxides $HOBr$ is formed and converted to Br by photolysis,



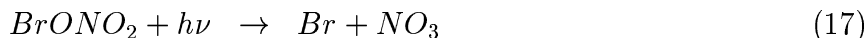
and a similar pathway was recently pointed out for CH_3O_2



The reaction rate coefficient of BrO with CH_3O_2 is about the same as for HO_2 .

In a possible branch of the $BrO + HO_2$ reaction HBr and O_3 may be formed. This branch is not accounted for in the scheme, but if it exists it influences the partitioning of reactive and unreactive bromine greatly. Garcia and Solomon (1994) examined the effect of different branching and found the BrO abundance to depend critically on the yield of HBr . Comparisons between model calculations and observations suggested a yield substantially less than 5%. Laboratory measurements by Poulet et al., 1992 pointed out the fact that HBr is a possible product of the $BrO + HO_2$ reaction, but suggested a negligible yield at 298 K. Mellouki et al., 1994 suggested that at most 0.01% of the $BrO + HO_2$ reaction would give HBr as a product.

Burkholder et al., 1995 pointed out that if $BrONO_2$ photolysis produced NO_3 and Br an effective $BrONO_2$ cycle may exist through:



where either photolysis of $BrONO_2$ or of NO_3 is the rate limiting step. However the products of $BrONO_2$ photolysis is rather uncertain, and if BrO and NO_2 are produced instead of Br and NO_3 the cycle will be a null cycle.

When only gas phase chemistry is accounted for box model studies have shown that this reaction chain may in many cases slightly suppress O_3 depletion since in the absence of this chain more BrO would have been available to react with HO_2 to make $HOBr$ which photolyze more rapidly back to active Br than $BrONO_2$ does.

The role of Cl_2 emissions is more complicated than the role of bromine. Box model calculations which represent the role of chlorine in polluted and clean air were performed. Table 1 gives the emissions and initial concentrations used in the runs. The scenario of polluted air was performed by assuming that a parcel of air was advected over land for three days exposed to emissions (see Table 1) and thereafter entering into the marine environment without emissions of non-halogenated species and with constant emissions of Br_2 and Cl_2 for five days. In addition a clean air scenario was performed by assuming a parcel of air being in a marine environment for five days without any emission of non halogenated species and constant emissions of Br_2 and Cl_2 . All emissions were assumed to be instantaneously mixed in the boundary layer with a height of 1000 m.

Calculations were done with different emission rates of Br_2 ranging from 3.5×10^8 molecules $cm^{-2}s^{-1}$ (0.5 ppt/h) to 1.0×10^{10} molecules $cm^{-2}s^{-1}$ (15 ppt/h). Figure 2 shows the reduction of ozone with increased Br_2 emissions after two and five days in the polluted and clean air case. Peak BrO concentration calculated with no Cl_2 emissions within the five days ranged from 2.9 and 4.5 ppt in the polluted and clean air cases, respectively, to 45.3 and 46.7 ppt for zero chlorine emissions. It is seen that in the absence of chlorine the rate of destruction increase with increasing Br_2 emission.

species	Initial conc.		emissions	
	clean	polluted	over land	over sea
O_3	30	40	0	0
H_2O_2	2.0	2.0	0	0
NO	0.1	0.2	5.0×10^{11}	0
NO_2	0.2	0.5	0	0
HNO_3	0.1	0.1	0	0
CO	100	200	1.4×10^{11}	0
H_2	500	500	0	0
SO_2	0.1	0.2	1.4×10^{11}	0
CH_4	1700	1700	0	0
C_2H_6	2.0	3.0	$0.45 * 1.0 \times 10^{12}$	0
C_2H_4	1.0	1.0	$0.30 * 1.0 \times 10^{12}$	0
C_2H_2	0.2	1.0	$0.10 * 1.0 \times 10^{12}$	0
CH_3OH	0.5	1.0	$0.10 * 1.0 \times 10^{12}$	0
$HCHO$	0.1	1.0	$0.05 * 1.0 \times 10^{12}$	0

Table 1: Initial concentrations (ppb) and emissions (molecules $cm^{-2}s^{-1}$) used in the box model calculations.

Runs including Cl_2 emissions ranging from 1.0×10^{10} molecules $cm^{-2}s^{-1}$ (15 ppt/h) to 8.0×10^{10} molecules $cm^{-2}s^{-1}$ (120 ppt/h), were performed to investigate the influence of chlorine chemistry on the bromine compounds and on the ozone depletion. Peak ClO concentrations ranged from 11 to 88 ppt in the polluted case and 26 to 68 ppt in the clean air case when no

bromine was emitted. When bromine emissions was included the ClO concentrations dropped significantly due to the reactions with BrO .

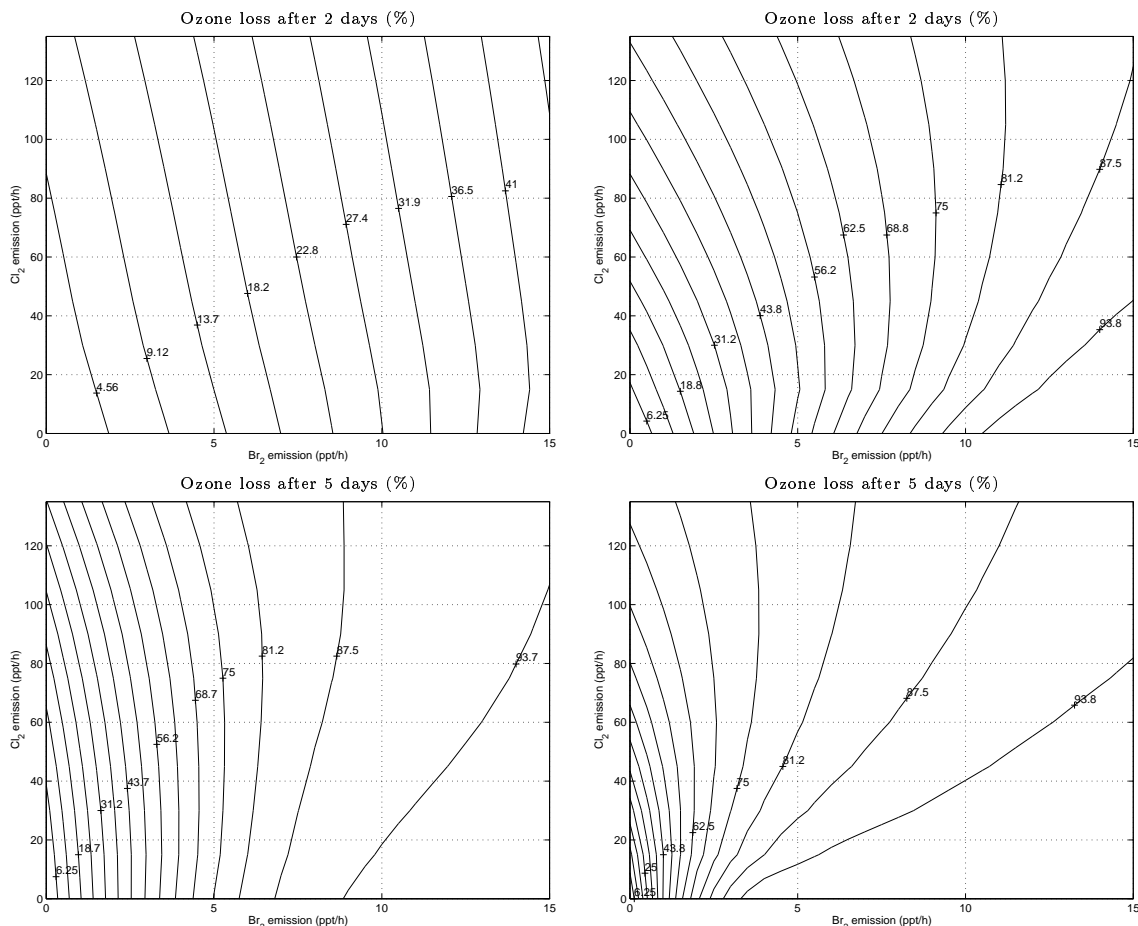


Figure 2: Isolines for ozone loss in % compared to a case with zero halogen emissions after 2 and 5 days of emissions of Br_2 and Cl_2 in the polluted (left) and clean air case (right).

Figure 2 shows that the role of Cl_2 emissions is more complicated than the role of bromine. The formation of ClO will influence the ozone destruction in a quite nonlinear way. The ozone destruction rate increases through the photolysis of Cl_2 :

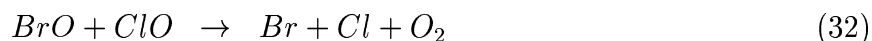


There are several less important reaction products of the ClO self reaction (See Table 3).

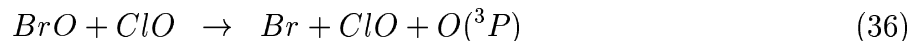
The chlorine compounds will also affect the destruction efficiency of Br through the coupling of BrO and ClO through three different routes:



where below 15 km formation of $BrCl$ is the rate limiting step (Lary, 1996). This cycle is about six times slower than the alternative cycle:

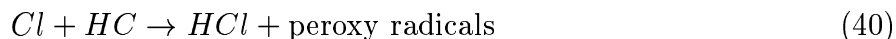


One branch of the $BrO + ClO$ reaction gives ClO and $O(^3P)$, which is almost as fast as the cycle above. This cycle gives no net ozone loss:

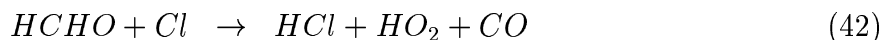
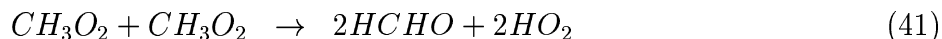


In the two latter cycles the rate limiting step is the $BrO + ClO$ reaction.

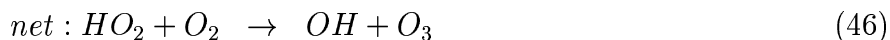
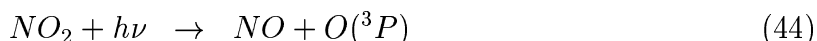
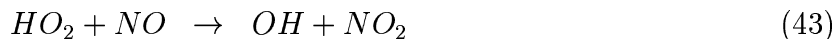
The $BrO + ClO$ reaction 35 is about three times faster than the BrO self reaction which means that even if small amounts of ClO is present the $BrO + ClO$ reactions may be important. This may reduce the ozone destruction efficiency of $BrO + BrO$ in favor of $BrO + ClO$ which at most will give one Br and one Cl atom. Even if the reaction rate coefficient of Cl with ozone is higher than that of Br , there are more competing reaction pathways for Cl due to its higher reactivity with hydrocarbons.



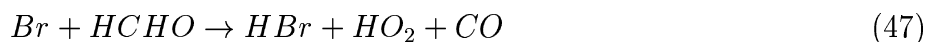
which may reduce the total ozone depletion compared to the case of no Cl_2 emission. In addition to be a sink of reactive Cl the reactions with hydrocarbons may also increase the peroxide concentration which may have one of two effects on the ozone concentration:



HO_2 can then be converted by NO into OH and produce a further molecule of ozone:



or remove ozone through the $HO_2 + O_3$ reaction. The importance of these reactions depends on the NO_x level. Chlorine compounds will greatly influence the $HCHO$ concentration through the enhancement of peroxides (eg. reaction 41). The increase in $HCHO$ can reduce the effect of bromine induced ozone destruction since a greater portion of the bromine will be in an unreactive form through



which in this scheme is the most important sink of active bromine.

This makes the total O_3 destruction potential for the coupled bromine and chlorine chemistry highly nonlinear and dependent on both the bromine to chlorine emission ratio and the concentration level of other compounds.

3 Model calculations with the UiB 3-D model

The fate of the halogens released in the marine environment was investigated by implementing the gas phase chemistry scheme in Table 3 in a 3-D model and calculations were done for the period 30 April - 10 May 1997 which coincides with measurements done at Mace Head (see section 4).

Since both source strength and origin are not well known, these calculations will only indicate the effect of halogens. The relative importance of the different physical and chemical processes involved is emphasized and the partitioning among the different halogen compounds will be discussed.

3.1 Model description

The Mesoscale Chemistry Transport (MCT) model is developed at the University of Bergen (Flatøy, 1994). It is an Eulerian chemistry-transport model with 10 unequally spaced vertical layers up to 100 hPa with a horizontal grid resolution of 150 km at 60° N. The general approach used in the model is similar to that of the regional acid deposition model RADM (eg. Chang et al., 1987) developed at NCAR. Special attention is made to the treatment of stratiform and convective cloud and precipitation processes (Flatøy, 1992).

The meteorological data necessary to run the model are provided by a weather prediction model (NWP) based on the limited area model Lam50 from the Norwegian Meteorological

Institute (Grønås et al.,1987 and Nordeng, 1986). The NWP model has an extended treatment of clouds and precipitation (Sundqvist, 1988, Sundqvist et al.,1989 and Kvamstø, 1992).

The physical exchange processes are treated as advection and diffusion. Transport in convective updrafts and wet and dry removal are described. A second order version of the advection scheme proposed by Bott (1989) is used to solve the advective part. By using a method by Strand and Hov (1993) the Bott scheme can be used in sigma coordinates with variable spacing in the vertical.

The diffusive part is solved using a semi implicit Crank-Nicholson scheme centered in time with an eddy diffusion coefficient K_z with a parameterization based on the stability in the atmospheric boundary layer. For the surface layer (lowest model level) K_z is given as

$$K_z = ku_*z(1 - \frac{z}{h})^2/B(\frac{z}{L}) \quad (48)$$

where k is von Karman's constant, u_* the friction velocity and B non-dimensional concentration profiles (Businger et al., 1971) which vary with stability. When the air is stable or neutral this formulation is also used in the rest of the boundary layer. During unstable conditions, however, growth of convective plumes is the dominant process and K_z is computed as

$$K_z = kw_*z(1 - \frac{z}{h}) \quad (49)$$

where the convective velocity w_* has replaced the friction velocity. Above the boundary layer K_z is calculated as

$$K_z = K_{z,0} + l^2 \cdot \left| \frac{\Delta v}{\Delta z} \right| \cdot \frac{(R_c - R_b)}{R_c} \quad (50)$$

where $K_{z,0}$ is the background value $1.0 \text{ m}^2\text{s}^{-1}$, l the mixing length, Δv the horizontal wind speed difference across the layer of thickness Δz , R_b the Richardson number and R_c the critical Richardson number given as $R_c = 0.257 \cdot \Delta z^{0.175}$. K_z is set equal to $K_{z,0}$ if the Richardson number gets larger than the critical value. A more detailed description can be found in Strand and Hov (1993) and Flatøy (1994).

The convection is calculated by a modified version of the Asymmetrical Convective model (ACM) by Pleim and Chang (1991). The ACM is a simple non-local closure model for vertical mixing in the convective boundary layer (CBL), based on the assumption that the vertical transport within the CBL is inherently asymmetrical. The ACM simulates the rising buoyant air plumes originating in the surface layer by moving air parcels from the lowest layer directly to the other layers in the CBL. The compensating downward motion takes place from one layer to the layer below, in order to simulate the slow subsidence surrounding convective plumes. This scheme gives faster upward transport of the surface emission compared to the normal eddy diffusion.

The MCT is designed to study the atmospheric chemical processes in the troposphere and aims at simulating the main parts of the observed tropospheric photochemistry. In this study the bromine and chlorine chemistry and the simplified hydrocarbon chemistry with lumped species discussed in section 2 are used.

The photolysis rates are calculated for a typical mid latitude spring/summer atmosphere (Anderson et al., 1986) with a background aerosol load using a albedo of 0.1. The program used is the Phodis program package (Kylling et al., 1995) which calculates photodissociation rates in the wavelength range 116-850 *nm* with optional cloud and aerosol calculations. The radiative transfer calculations are done for three regions, including 202.5-850.0 *nm*, with multiple scattering to account for O_2 , O_3 , Rayleigh scattering and optional water clouds, cirrus clouds and aerosols. The handling of multiple scattering may be done in different ways in the Phodis package. In this calculation a two-stream algorithm was used (Kylling et al., 1995). Absorption cross sections were collected from the literature. Typical daytime photolysis rates are given in Table 4. 21 different photolysis rates J_i (see Table 4) are computed for each grid box from the function

$$J_i = a_i \exp(-b_i \sec\theta) \quad (51)$$

where θ is the zenith angle and a_i and b_i precomputed values computed by the radiative transfer model. Typical values are given in Table 4.

The dry deposition of O_3 , H_2O_2 , NO_2 , HNO_3 , CH_3O_2H , CO , HCl , $HOCl$, HBr , $HOBr$ and SO_2 is included in the model as a function of latitude, time of day, time of year, biological activity of the surface, surface type and meteorological conditions. The formulations applied are similar to descriptions found in McKeen et al. (1991) and Hass (1991) and maximum deposition velocities over land and sea are given in Table 5. Wet deposition of HNO_3 , SO_2 , H_2O_2 , CH_3O_2H , HCl and HBr is calculated from the rate of precipitation at ground, the rainout rate from each vertical layer available from the numerical weather prediction model, and the wet scavenging coefficient for each species (Table 6).

Emissions of anthropogenic NO_x and $NMHC$ were taken from the CORINAIR 50·50 km^2 inventory for 1993. In the calculations the anthropogenic $NMHC$ emissions were represented (by volume) as 45% ethane, 30% ethene, 10% ethyne, 10% methanol and 5% formaldehyde. The chemistry and emissions of isoprene end terpenes are not taken into account since their reactions towards halogens are unknown and they are assumed to have only minor direct influence in the marine environment due to their short lifetimes.

3.2 Model results and discussion

Calculations were done for the period 28 April - 10 May 1997 (result for the first two days considered as spin up and not used) to investigate the competition between chemical and physical processes in the determination of the fate of the halogen radicals, to assess the importance of the various processes that determine the partitioning between different halogenated compounds and the potential role of halogens in the oxidation of $NMHC$, NO_x and ozone in the marine environment.

Only gas phase chemistry was considered and emissions of Br_2 and Cl_2 were prescribed to keep the BrO and ClO concentrations near the detection limit of previous measurements done with DOAS instruments. The emission rates chosen were 3.5×10^8 and 1.0×10^{10} molecules $cm^{-2}s^{-1}$ of Br_2 and Cl_2 , respectively, over the sea (no emissions over ice and land) and emitted

in the lowest model layer (0-90 m). Constant emission rates were assumed due to lack of more information, but the fate and concentration range of the different halogen compounds over different areas and under different meteorological conditions could then be investigated. Since the main aim of this study is to investigate the relative importance of halogens and their partitioning, zero cloud cover was assumed to facilitate the investigation of the change in chemistry with latitude.

In Figure 3 the mean sea level pressure and wind in model layer 8 (~ 1200 m) are shown.

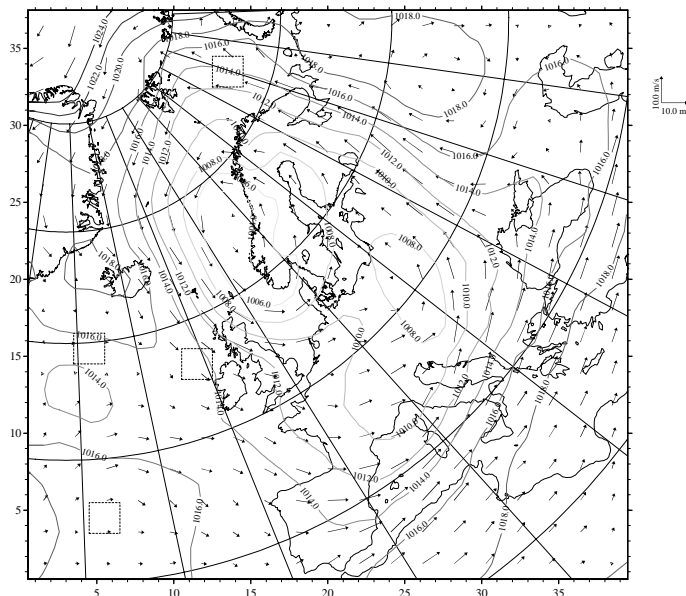


Figure 3: Mean sea level pressure and mean windspeed at model level 8 (~ 1200 m) for model period 30 April - 10 May 1997.

The period was characterized by a rather weak low pressure system west of Norway and a high pressure ridge in the south Atlantic. Surface winds were very low in the south western part of the model area with winds on average being 2-3 m/s and gusts up to 7-9 m/s. On the other hand winds north west of the UK were on average 8-10 m/s with gusts up to 20 m/s west of Ireland.

Figures 4 and 5 give the average concentration of BrO , total gas phase bromine ($BrO_y = Br + 2 \cdot Br_2 + BrO + HBr + HOBr + BrONO_2 + BrCl$), ClO and total gas phase chlorine ($ClO_y = Cl + 2 \cdot Cl_2 + ClO + HCl + HOCl + ClONO_2 + 2 \cdot Cl_2O_2 + BrCl$), respectively, in the lowest model layer (0-90 m) over the model domain when no heterogeneous or aqueous phase reactions were considered. Even if the emissions of halogens were held constant over the sea the average BrO_y and ClO_y concentrations vary with almost an order of magnitude from 3 to 20 ppt and from 70 to 650 ppt, respectively, within the model domain. The highest concentrations

were found in the south western part of the model domain. This is explained by low windspeeds and little vertical diffusion in this area allowing a larger portion of the halogens to stay near the surface. A more comprehensive explanation and partitioning of the total bromine and chlorine concentrations into different compounds are given in section 3.3.

Figures 6 to 10 give the average concentration during the 10 days model period and difference between a run with halogen emissions and one without (with halogens/no halogens) of ozone, *NMHC*, *HCHO* and NO_x and average 12 GMT concentrations of RO_2 ($HO_2 + CH_3O_2$) in the lowest model layer (0-90 m).

It is seen that the east and north east Atlantic and the North Sea area are characterized by low concentrations of both primary and secondary pollutants due to the westerly and north westerly winds bringing clean air into this area. In the areas with high chlorine concentrations, on average 15% more of the *NMHCs* were oxidized giving an increase in *HCHO* and daytime RO_2 of around 30% where the *ClO* and *ClO_y* concentrations are highest. In this area the *ClO* concentrations then peaked up to 10-30 ppt during sunrise. This reduction in *NMHCs* and increase *HCHO* concentrations have also been reported in the literature during arctic ozone depletion events (Ramacher et al., 1997 and De Serves, 1994). Also a large relative reduction of NO_x is seen with reductions of around 50% in these areas where *HCHO* and RO_2 increased. This is mainly due to production of *ClONO₂* from the reaction of *ClO* with NO_2 . Reduction of NO_x in the presence of halogens is supported by observations of NO_x reported by Beine et al. (1997) for Arctic conditions. A more thorough description of the halogens influence on other compounds in the different areas is given in section 3.5.

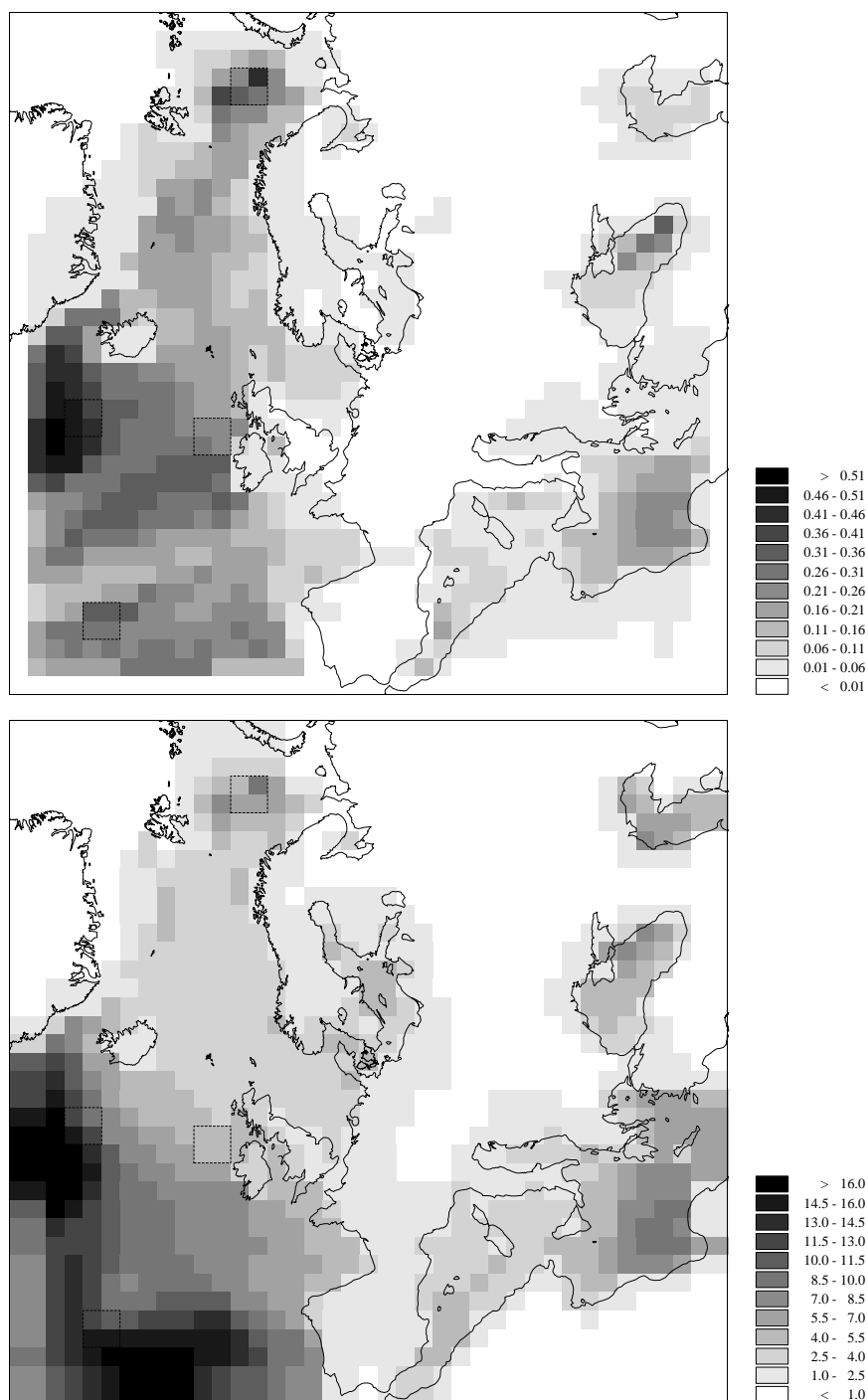


Figure 4: Average BrO (upper) and average BrO_y (lower), (ppt) in the model domain during the model period (30 April - 10 May, 1998) for the lowest model layer (0-90 m). Due to ice north east of Greenland no halogens were emitted in this region.

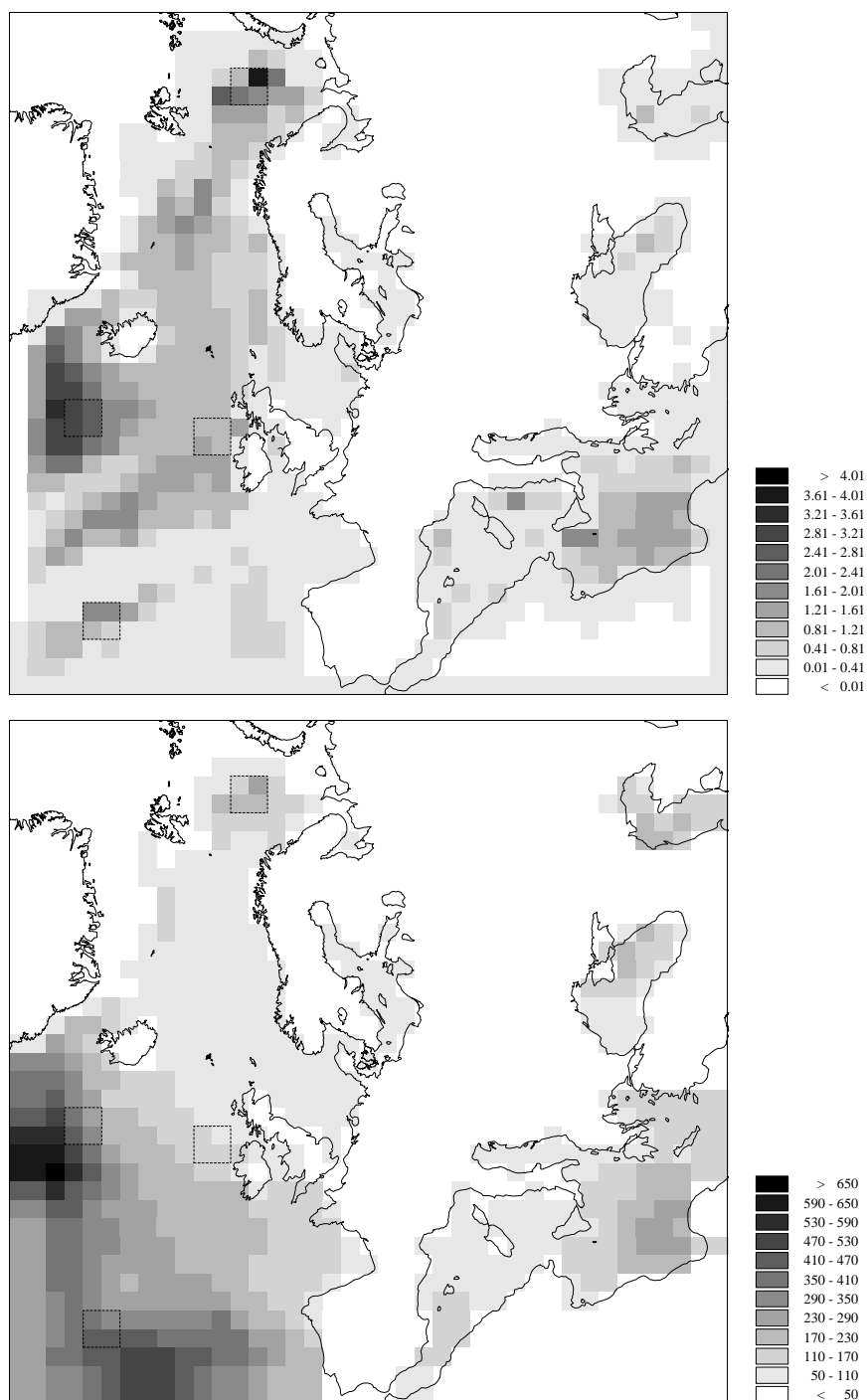


Figure 5: Average ClO (upper) and average ClO_y (lower) (ppt) in the model domain during the model period (30 April - 10 May, 1998) for the lowest model layer (0-90 m). Due to ice north east of Greenland no halogens were emitted in this region.

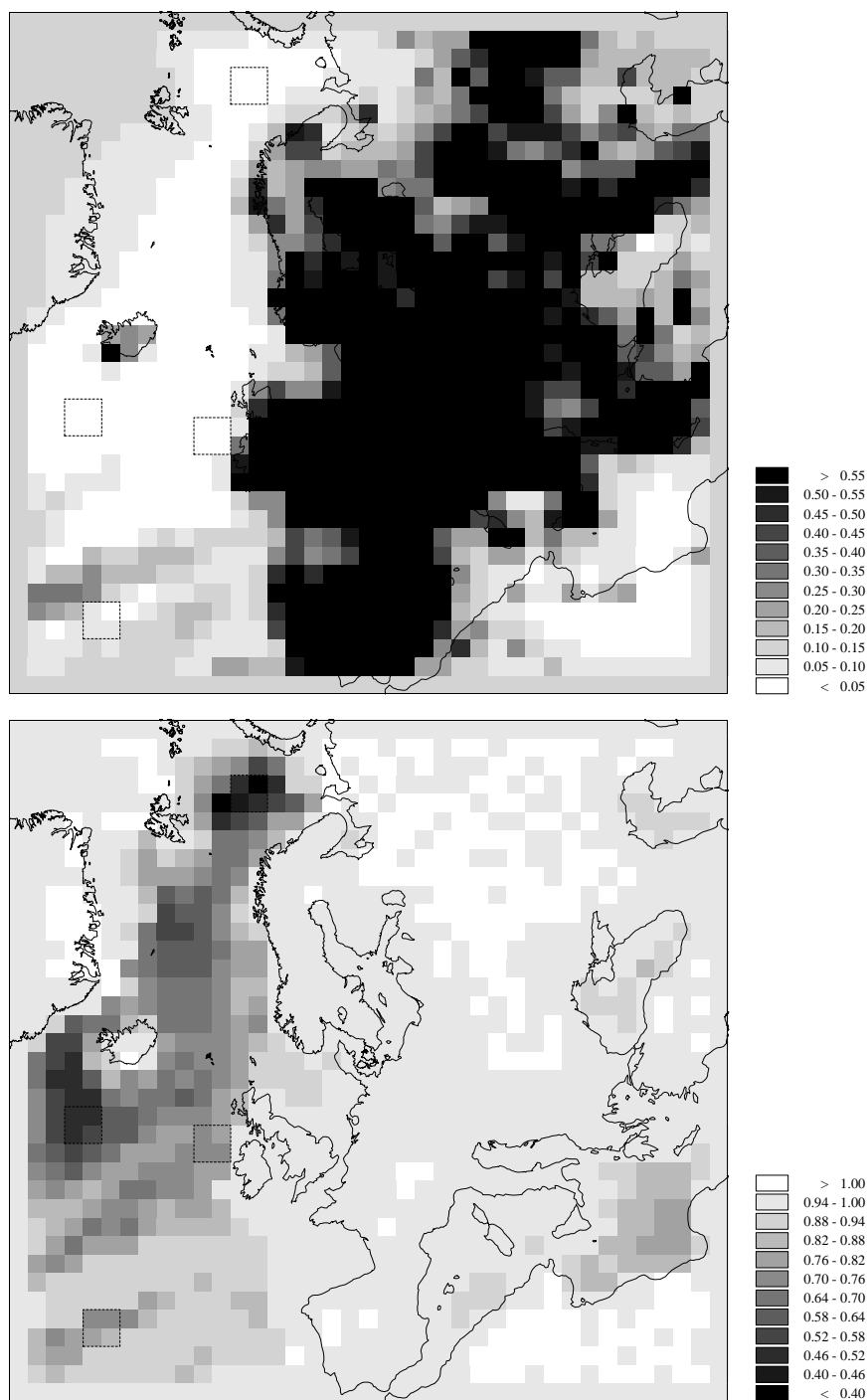


Figure 6: Average NO_x (upper) concentrations in ppb during a model run with halogen emissions and comparisons with a run without halogens (with halogens/no halogens) (lower).

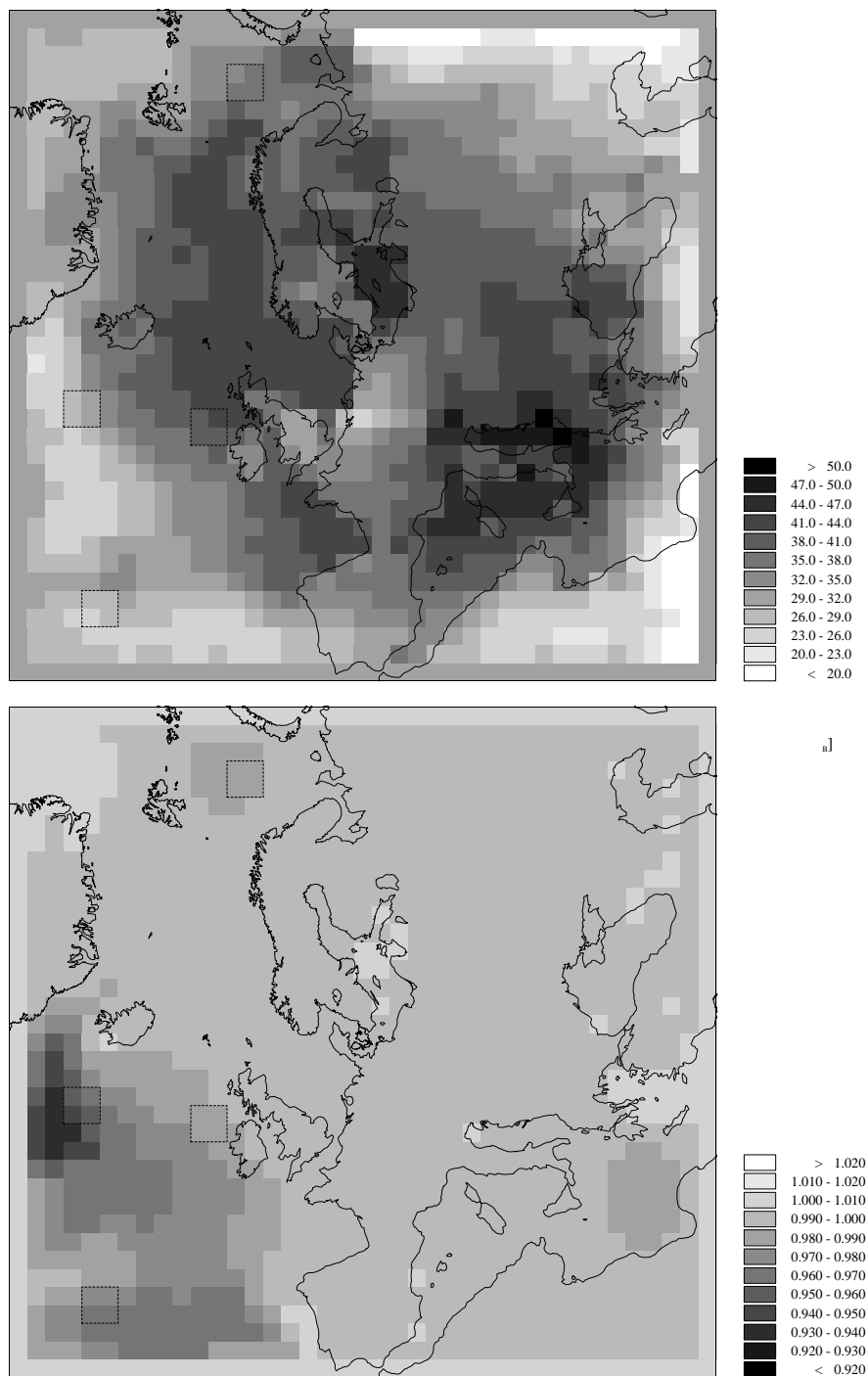


Figure 7: Average ozone (upper) concentrations in ppb during a model run with halogen emissions and comparisons with a run without halogens (with halogens/no halogens) (lower).

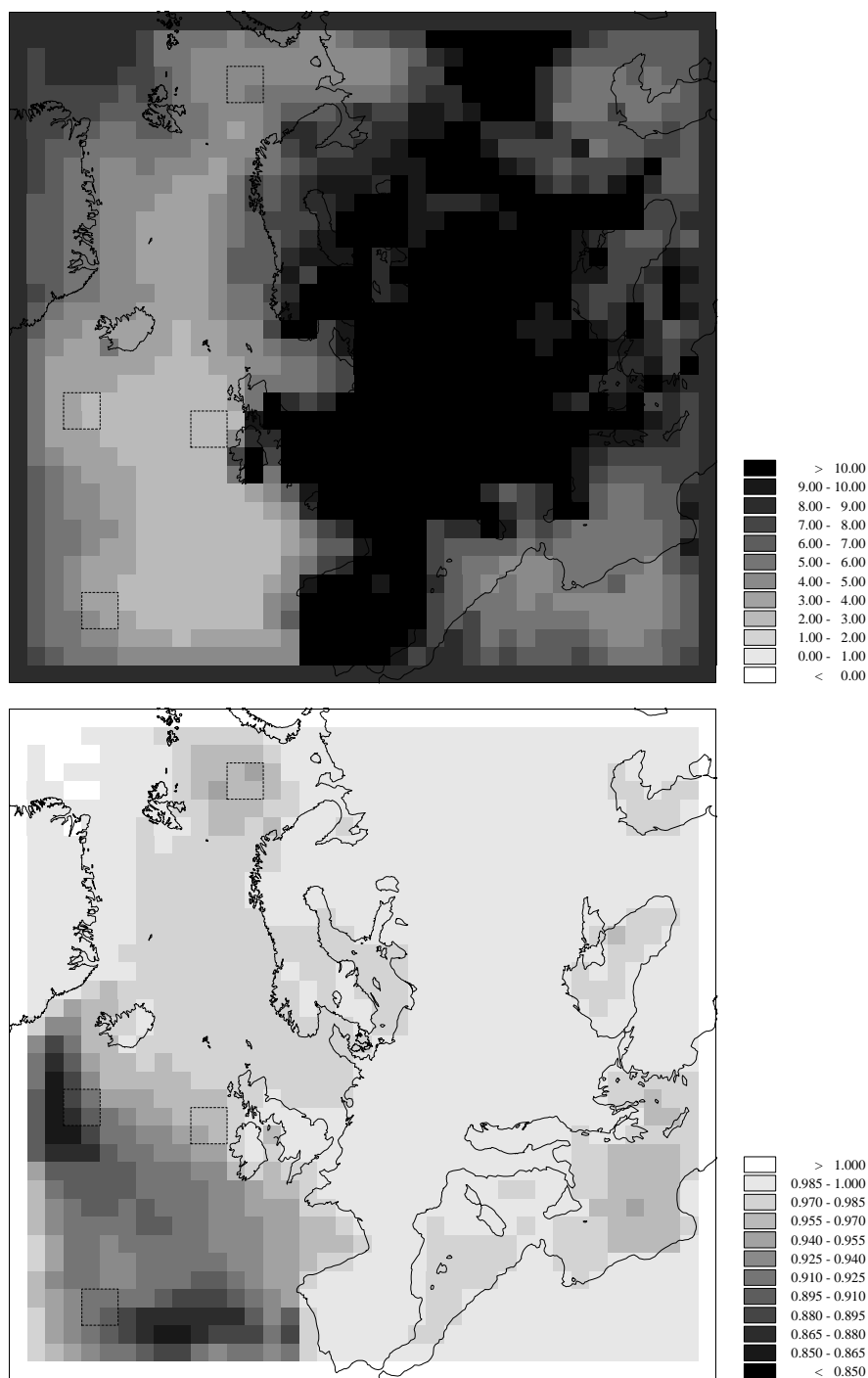


Figure 8: Average *NMHC* concentrations (upper) in ppbC during a model run with halogen emissions and comparisons with a run without halogens (with halogens/no halogens) (lower).

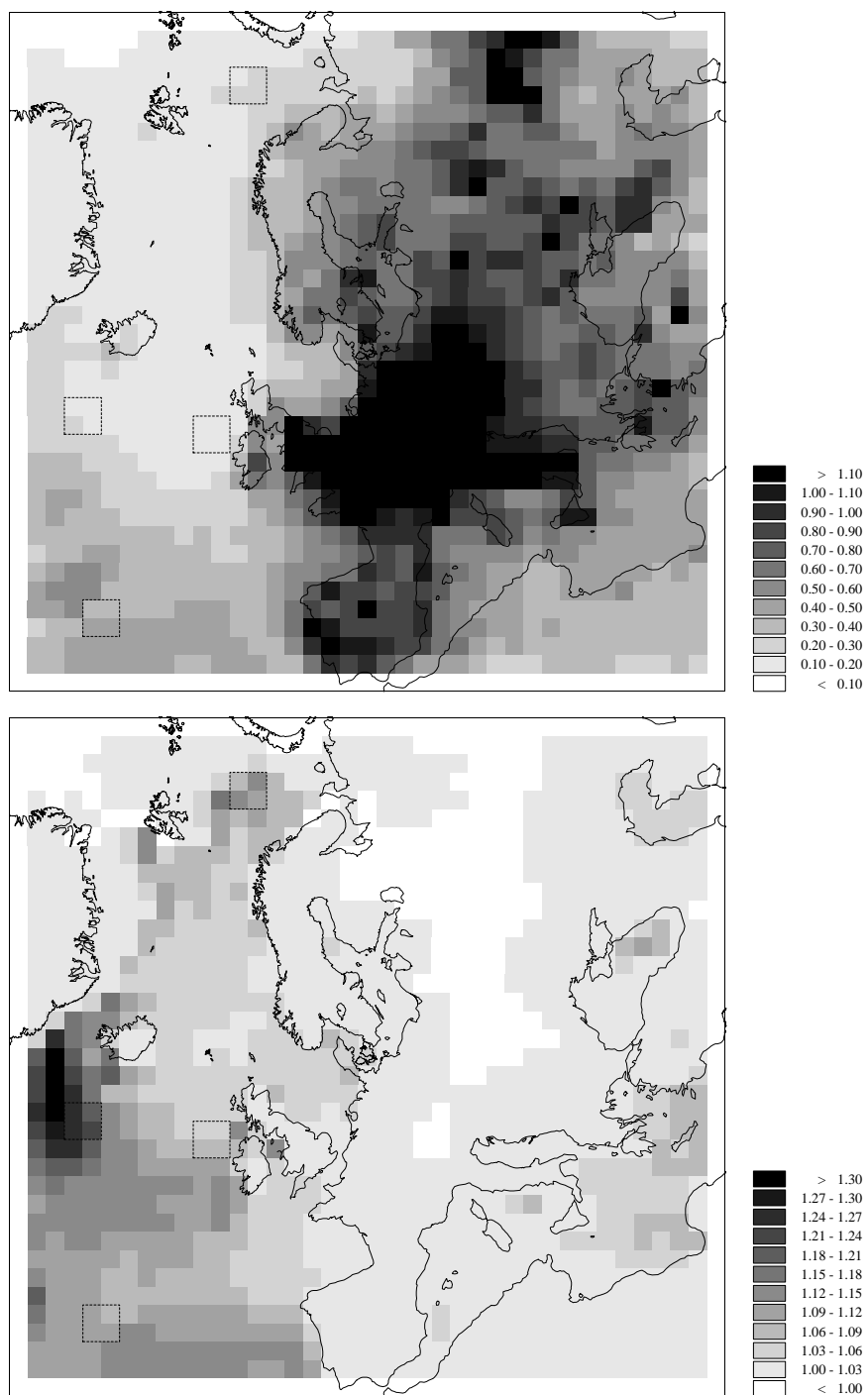


Figure 9: Average *HCHO* concentrations (upper) (ppb) during a model run with halogen emissions and comparisons with a run without halogens (with halogens/no halogens) (lower).

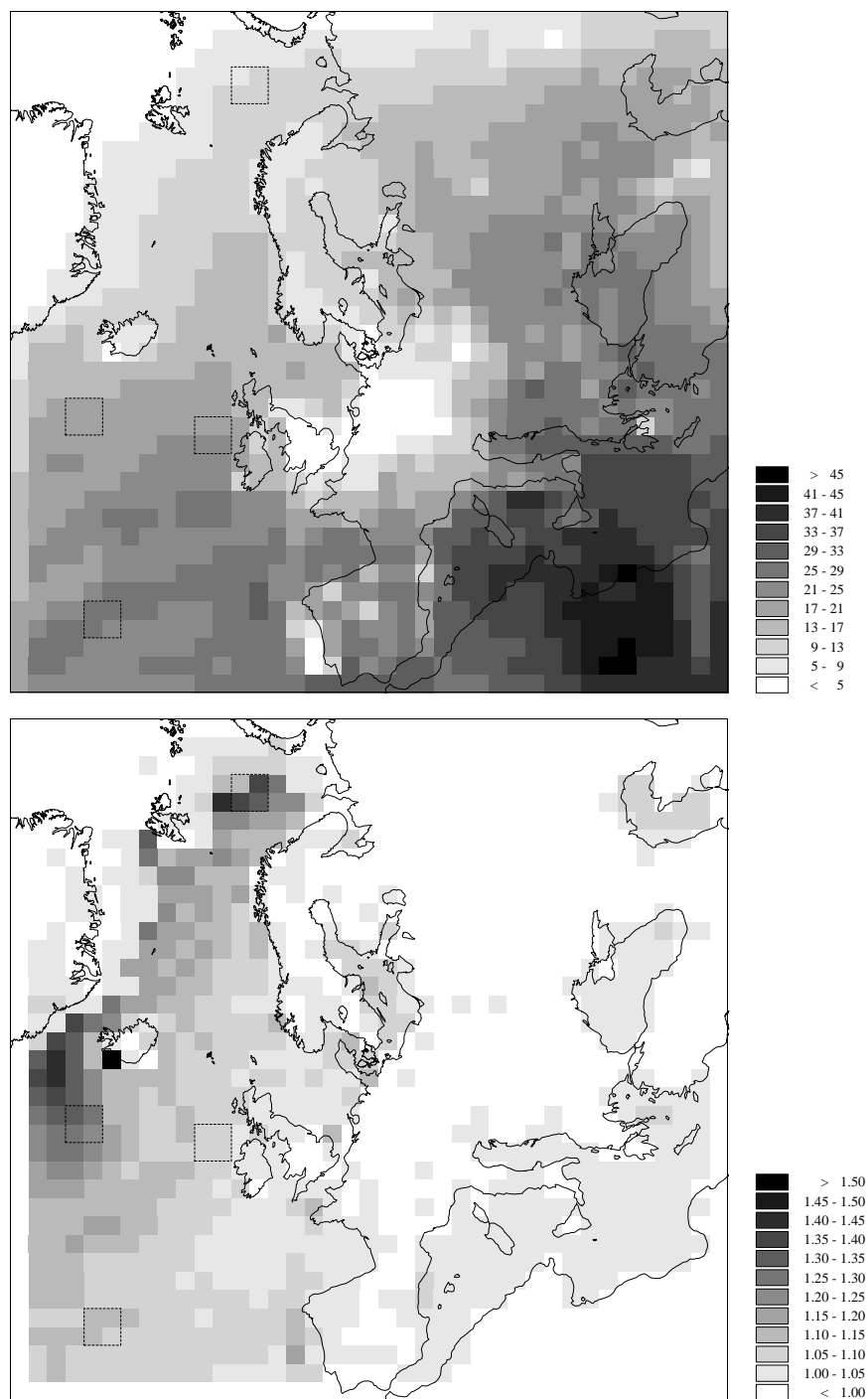


Figure 10: Average 12 GMT RO_2 concentrations (upper) in ppt during a model run with halogen emissions and comparisons with a run without halogens (with halogens/no halogens) (lower).

3.3 Partitioning and concentrations of the halogens over four sub areas.

Four sub areas (see Figure 3) of the model domain were chosen to show the differences in concentrations and partitioning of the halogens under different NO_x , VOC and ozone concentrations and different meteorological conditions.

All areas were characterized by low NO_x and hydrocarbon loads and quite similar levels of ozone. The windspeeds and temperatures were, however, quite different and this has led to large differences in the mixing of the halogens in the vertical.

- **Arctic:** Located at approximately 75° N with daytime temperatures around 0° C and an average windspeed of 5 m/s during the model calculation. Characterized by low NO_x (25 ppt), low $NMHC$ (5 ppbC), low RO_2 (12 ppt (average daily maximum)) and 35 ppb of ozone.
- **North Atlantic:** South west of Iceland at 60° N, daytime temperatures around 8° C and average windspeed 3 m/s. Low NO_x (15 ppt), low $NMHC$ (3 ppbC), medium RO_2 (18 ppt (average daily maximum)) and 29 ppb of ozone.
- **West of UK:** West of UK (56° N), daytime temperatures around 8° C and average windspeed 7 m/s. Low NO_x (25 ppt), low $NMHC$ (3 ppbC), medium RO_2 (21 ppt (average daily maximum)) and 40 ppb of ozone.
- **South Atlantic:** West of Spain (45° N), daytime temperatures around 15° C and average windspeed 3 m/s. Low NO_x (60 ppt), low $NMHC$ (4 ppbC), relatively high RO_2 (27 ppt (average daily maximum)) and 27 ppb of ozone.

3.4 Concentrations and partitioning of the halogen compounds

Figure 11 shows the concentrations of total bromine (BrO_y) and chlorine (ClO_y) and the individual bromine and chlorine compounds in the lowest model level for the four different areas.

The halogen emissions were constant in the calculation. The average BrO_y and ClO_y concentrations vary within a factor of 4 over the different areas, mainly due to differences in the vertical diffusion. This is seen in Figure 12 where the tendency terms in ppt/h for the different meteorological and chemical processes are calculated for the emitted specie Br_2 in the lowest model layer. Negative values indicate loss of the compound. The tendency terms describe chemistry+emission, horizontal advection, vertical advection, diffusion and convection. Due to the formulation of the numerical solution the chemistry and emission tendencies are not separated. On average 0.13 ppt/h is transported out of the lowest model layer by diffusion in the area west of the UK compared to 0.03 ppt/h in the north and south Atlantic area. This is a factor of about 3 and explains the differences in BrO_y and ClO_y concentrations in the different areas. In addition contributions by vertical and horizontal advection have to be taken

into account, but these two terms almost eliminate each other on average within the mixing layer when the emissions are uniformly distributed as here. This is, however, not always the case for shorter periods. It is also seen that the daily average maximum buildup of Br_2 due to emissions are 6-20 times the daily average. The buildup takes place during night and is reduced by photodissociation during daytime and may exceed the emission rates and therefore give a negative emission+chemistry tendency.

Due to higher emission rates and lower photodissociation rates more ClO_y remains as Cl_2 than is the case for BrO_y and Br_2 .

Since HBr and HCl are the two long lived reservoir components of bromine and chlorine in the gas phase, the HBr to BrO_y and HCl to ClO_y ratios express the amount of unreactive compounds available.

Figure 13 shows that HCl is on average 49 to 65% of the total chlorine, and up to 65-83% during daytime.

Due to much lower reactivity of Br with hydrocarbons, the HBr to BrO_y ratio is only 17 to 35%. The lowest ratio is in the Arctic area. This may be surprising since $NMHC$ and $HCHO$ are higher and OH lower (Figure 16) than in the other areas, favoring HBr production. But the photolysis of $BrONO_2$, $HOBr$ and BrO to Br is much slower in this region (75°N), and the production of HBr slower. This is also seen in the BrO to HBr ratio which is about 0.3, more than twice the value in the north and south Atlantic region. The low HBr to BrO_y ratio to the west of the UK is due to low $HCHO$ and $NMHC$ and high ozone concentrations compared to the other areas, favoring production of other bromine species.

Due to the high ozone and low $HCHO$ and $NMHC$ west of the UK, the BrO_x to BrO_y ratio is highest there (Figure 14) on average 6%. This is more than twice the value in the south Atlantic region.

Total bromine (BrO_y) is lowest in the area west of the UK, but the chemical production of BrO is largest, and on average 0.04 ppt/h, 3-5 times the average production in the other regions (Figure 15).

At night there is a net chemical loss of BrO since Br is low. BrO is removed by vertical diffusion to a larger extent than over the other regions and less remains to be chemically converted, causing a large chemical BrO production on average even if the daytime production is larger in all the other areas. The ClO_x to ClO_y ratio resembles that of BrO_x over BrO_y . Only 0.3 to 1% of total chlorine is found as ClO_x on average compared to 2.5-6% for BrO_x . BrO and ClO constitute over 95% of BrO_x and ClO_x .

3.5 The halogens influence on other compounds

The halogen emissions were rather small with daily BrO and ClO concentrations of only 0.3-0.5 and 0.5-1.1 ppt, respectively, with peaks up to 1.1-2.9 and 3-16 ppt, they had a pronounced effect on the clean air NO_x , $NMHC$ and RO_2 concentrations. Figure 16 shows that all areas have reduced $NMHC$ concentrations with 4-10%.

This increase in oxidation gave higher RO_2 and $HCHO$ concentrations. RO_2 increased by

5-28% with the largest increase in the Arctic. The RO_2 concentrations were lowest in the Arctic, and Cl reaction with hydrocarbons was most important there. The $Cl + \text{NMHC}$ reactions are temperature dependent, with faster reactions in a cold environment. Most of the RO_2 increase was due to increase in CH_3O_2 . Due to the increase in peroxy radicals a larger amount of $HCHO$ was produced by the CH_3O_2 self reaction. Also Cl reactions with CH_3O_2 and CH_3OH , and ClO reaction with CH_3O_2 , increased the $HCHO$ concentration. The reduction in average ozone concentrations due to the halogens were less than 1% (Figure17).

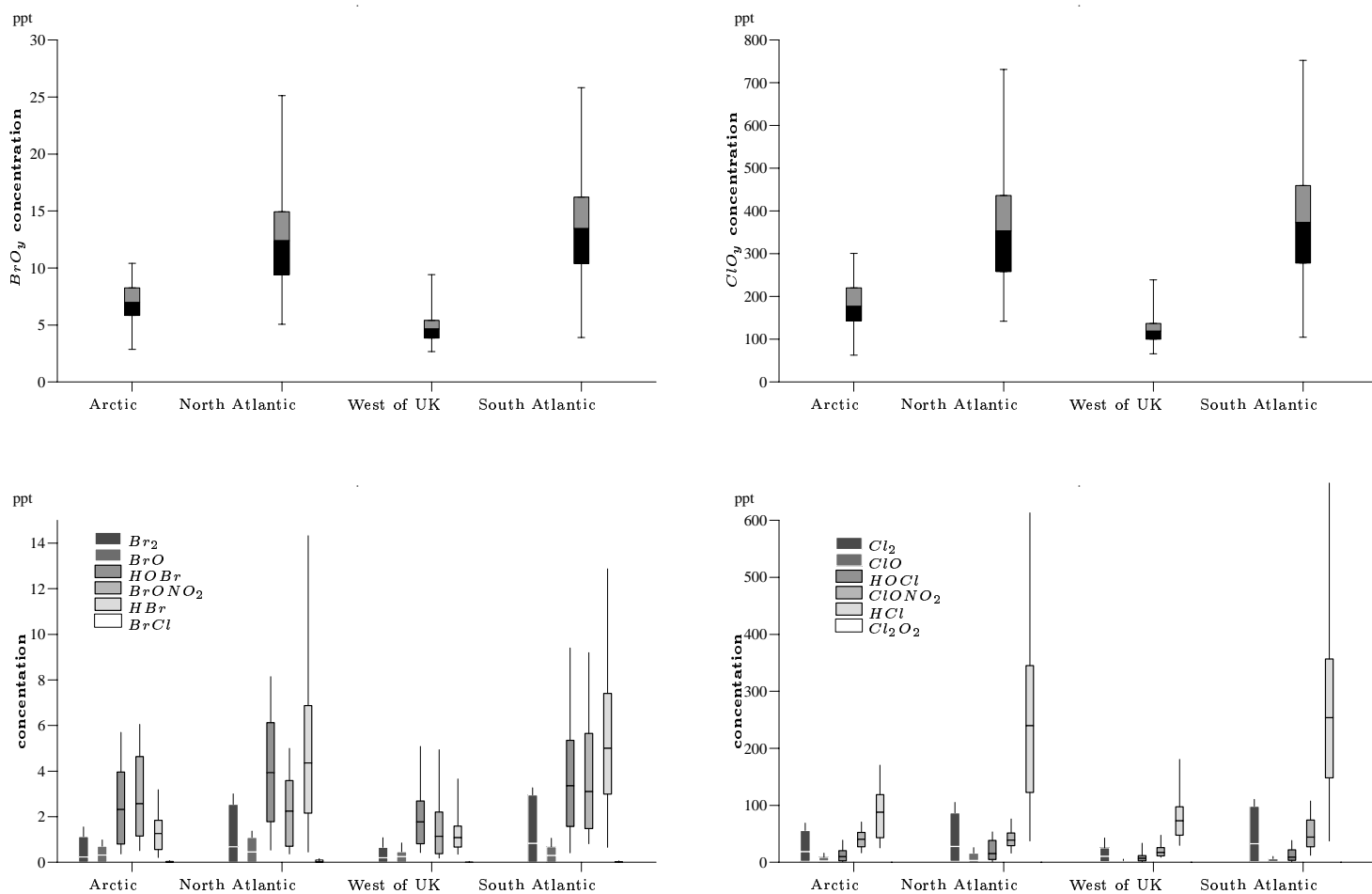


Figure 11: Average, daily average maximum, daily average minimum and maximum and minimum concentrations during the model period for total gas phase bromine (BrO_y , upper left) and chlorine (ClO_y , upper right) in ppt for the lowest model layer, and the concentrations of the individual bromine, (lower left) and chlorine (lower right) compounds (ppt).

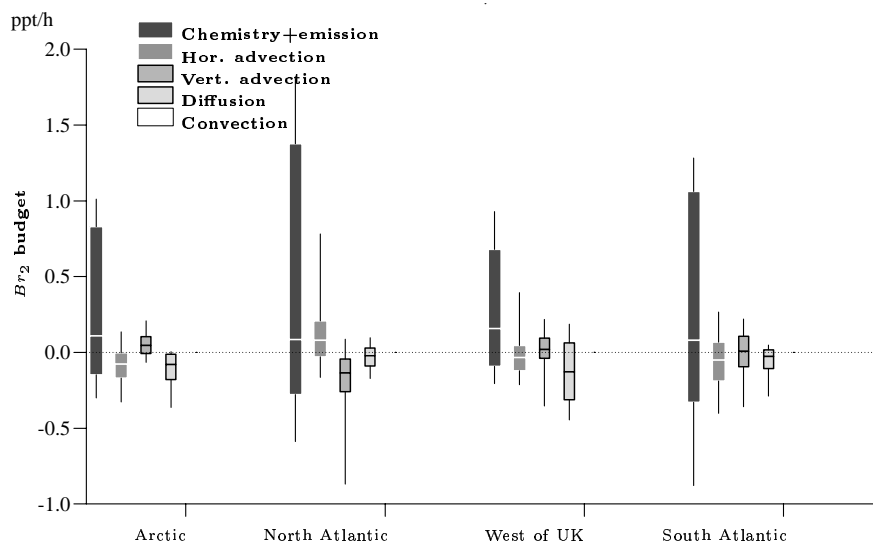


Figure 12: Average, daily average maximum, daily average minimum and maximum and minimum tendencies in ppt/h for the emitted specie Br_2 in the lowest model layer for the period 30 April - 10 May 1997.

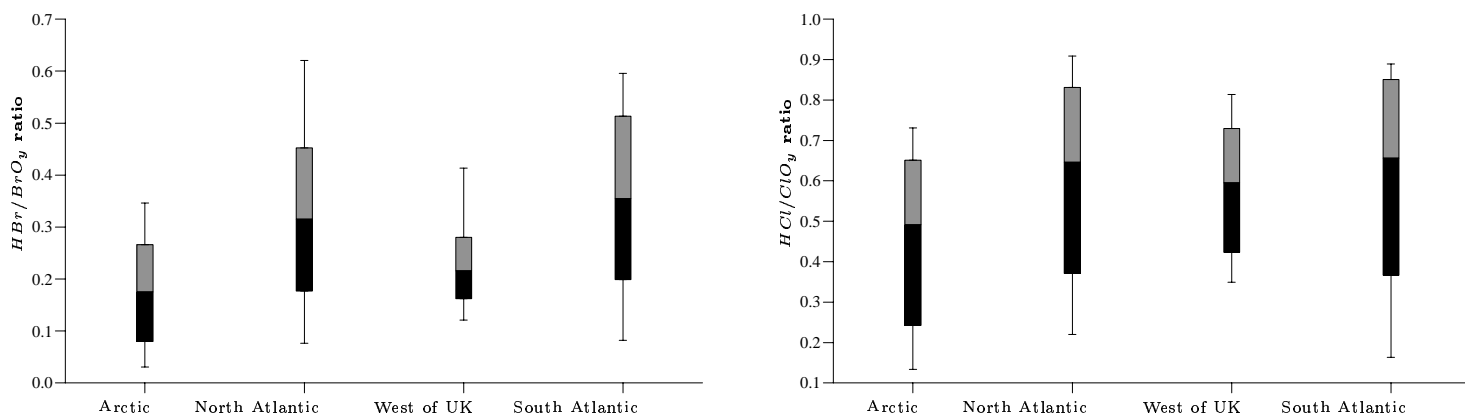


Figure 13: Average, daily average maximum, daily average minimum and maximum and minimum HBr/BrO_y (left) and HCl/ClO_y (right) over the four different areas for the lowest model layer for the period 30 April - 10 May 1997.

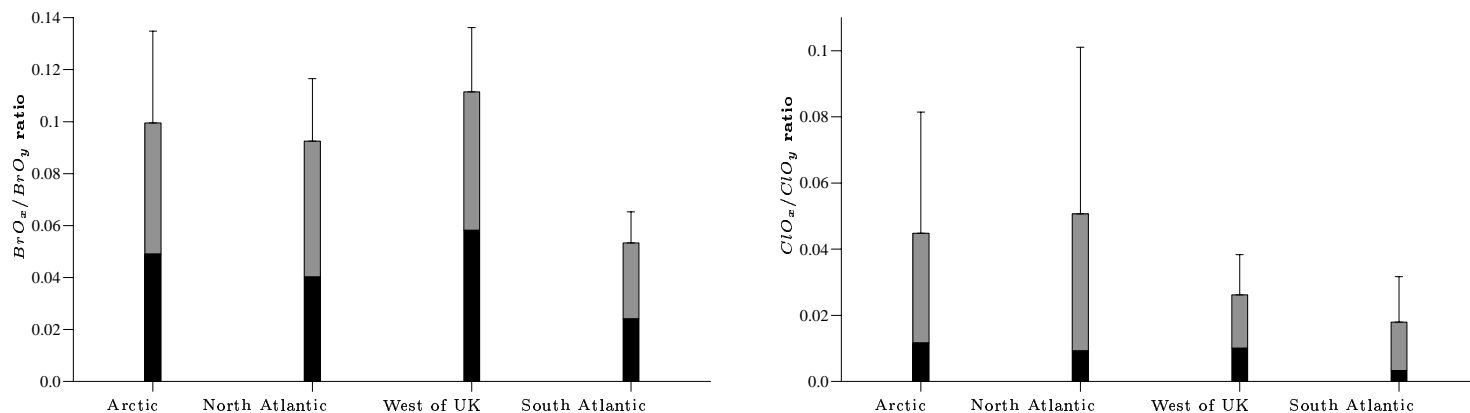


Figure 14: Average, daily average maximum, daily average minimum and maximum and minimum BrO_x/BrO_y (left) and ClO_x/ClO_y (right) over the four different areas for the lowest model layer for the period 30 April - 10 May 1997.

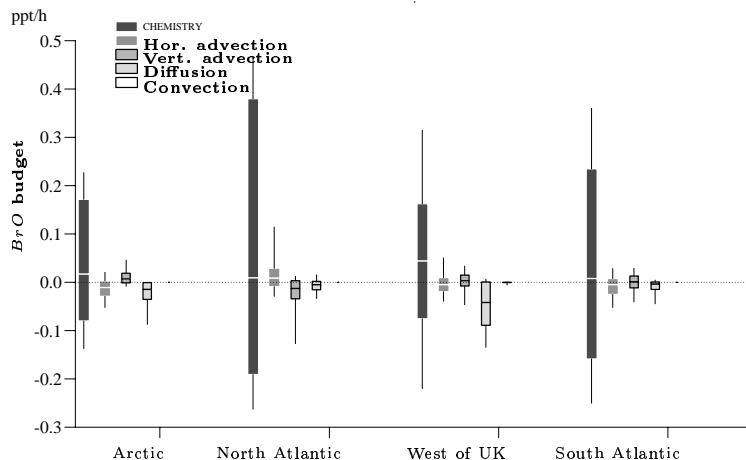


Figure 15: Average, daily average maximum, daily average minimum and maximum and minimum tendencies in ppt/h for BrO over the four different areas for the lowest model layer for the period 30 April - 10 May 1997.

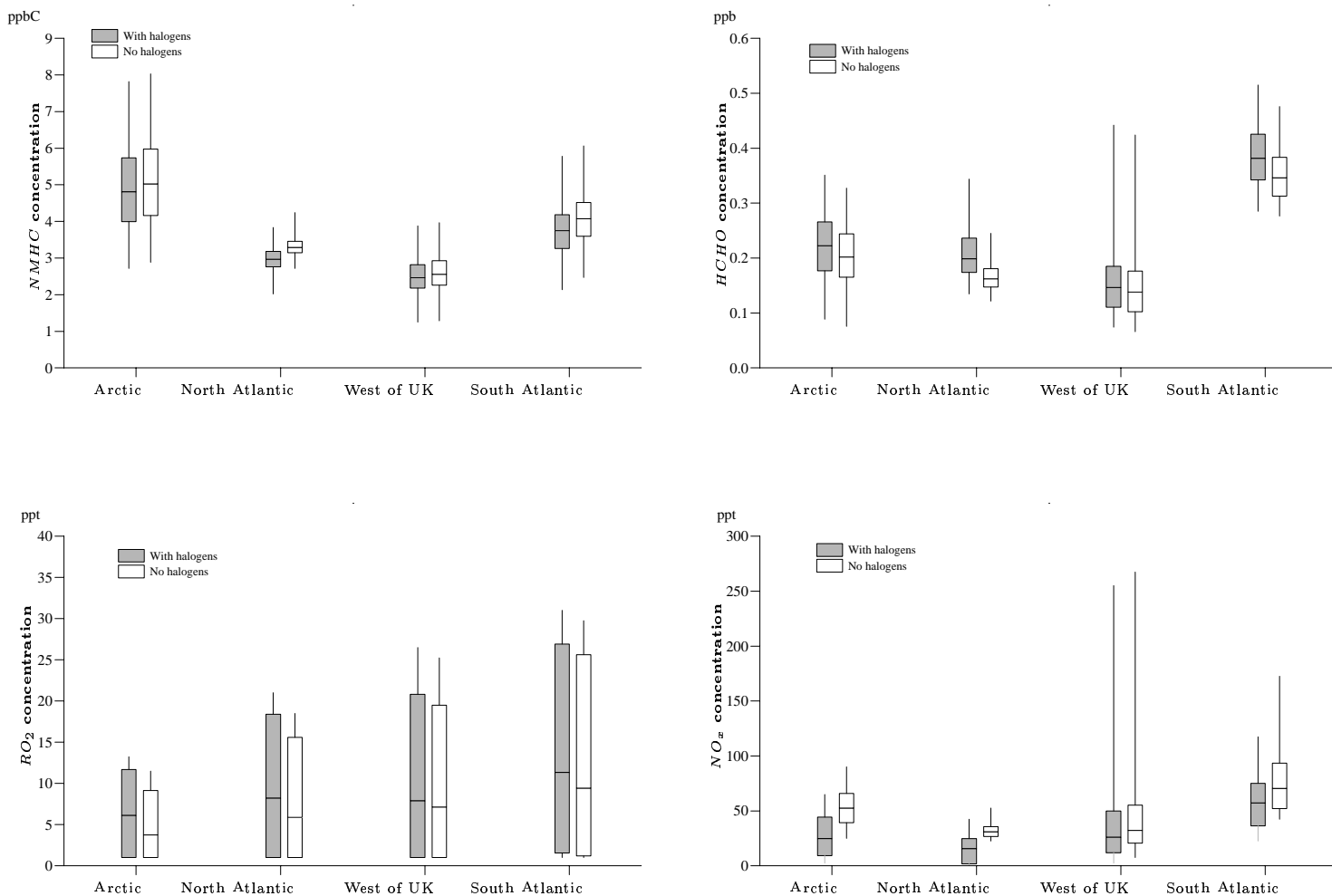


Figure 16: Average, daily average maximum, daily average minimum and maximum and minimum concentration of $NMHC$ (upper, left), $HCHO$ (upper, right), RO_2 (lower, left) and NO_x (lower, right) with (dark bars) and without (bright bars) halogen emissions for the period 30 April - 10 May 1997.

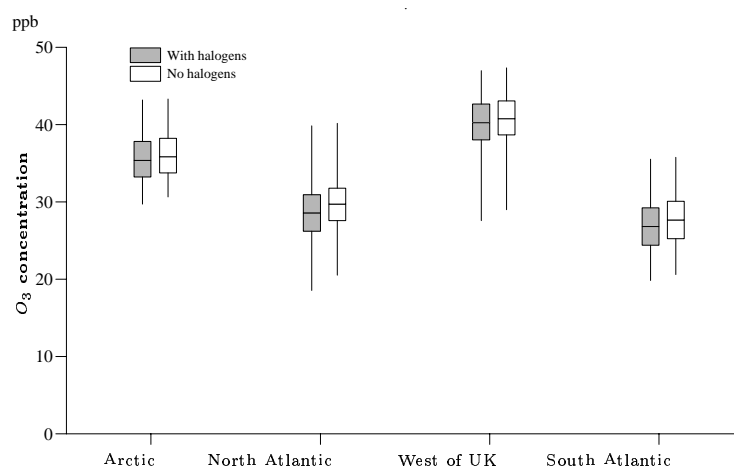


Figure 17: Average, daily average maximum, daily average minimum and maximum and minimum concentration of ozone with (dark bars) and without (bright bars) halogen emissions for the period 30 April - 10 May 1997.

4 Observations and model results

Most observations of tropospheric halogens are done in the Arctic environment (Hausmann and Platt, 1994; Tuckermann et al., 1997) and may not be directly comparable to the values calculated in this study, but they give an indication of the range of concentrations of halogens that might be found in the boundary layer. Table 2 summarizes observations of bromine and chlorine oxide during normal ozone levels and model calculations reported in this paper. The calculations reported here are within observed range of values for most cases.

Measurement campaign	<i>BrO</i>			<i>ClO</i>		
	AVG	PEAK	D.L.	AVG	PEAK	D.L.
	Measurements					
Polar Sunr. ¹	< 2.5	6	4			
ARCTOC 1995 ²	0.5	4	1.5	1.6	10	18
ARCTOC 1996 ²	0.8	7	1.5	1.3	10	4.5
Weybourne ³	0.035	3	2.6	1.5	30	14
Mace Head ⁴	-0.2	4.4	1.7			
	This model study					
3-D calc.	0.3-0.5	0.9-1.4		1.1-2.9	6-26	

Table 2: Average (AVG), peak levels (PEAK) and detection limit (D.L.) of measurements of *BrO* and *ClO* during periods of normal ozone concentrations and model calculations from the 3-D simulations done in this paper. The values cited for the model calculations is the concentration range for the four sub areas. ¹ Arctic polar sunrise experiment in Alert (1992), ² Arctic polar sunrise experiment in Ny Ålesund, ³Northfolk, UK (1996), ⁴western Ireland (1997).

There are few other measurements of other gas phase bromine and chlorine compounds. Perner et al. (1997) measured total gas phase bromine analyzed by neutron activation during the ARCTOC 1996 campaign, bromine to be around 10-20 ppt during normal ozone conditions. This is not directly comparable to the total gas phase bromine given in this study since organic bromine is not accounted for in the model, but in the 3-D calculations average *BrO_y* ranged from 7-13 ppt in the four different sub areas.

5 Conclusions

3D CTM case study were done to investigate the influence of low concentrations of halogens on ozone and precursors for the period 30 April to 10 May, 1997 over Europe and the North Atlantic. The period was characterized by clean air over the sea with small amounts of *NMHC* and *NO_x* in the range of 2-6 ppbC and 25-100 ppt, respectively. The emissions of halogens were held constant over the sea in order to investigate the differences in concentration levels do to mixing processes. *BrO_y* and *ClO_y* concentrations in the lowest model level varied with almost an order of magnitude within the model domain due to differences in vertical diffusion.

This shows that physical processes are important for the halogen concentrations, and observed increases in concentration may often not indicate increased emissions.

HCl was seen to be by far the most important *ClO_y* component and accounted for more than 50% of total *ClO_y* even if the hydrocarbon loads were quite small. In contrast, *HBr* accounted for about 20% of total *BrO_y*. Chlorine is thus much faster deactivated if no heterogenous or aqueous phase reaction reactivates *HCl*. The partitioning of the different bromine species was more similar than in the chlorine case and in some areas both *HOBr* and *BrONO₂* exceeded the *HBr* concentration on average.

ClO concentrations of a few ppt as a daily average, and with maxima of 10-30 ppt during daytime, oxidized 10-15% more of the *NMHCs* compared to a run without halogens. This increased the daytime peak of *RO₂* with 15-30% and increased the *HCHO* concentration on average 10-20%. The halogens were shown to have little effect on ozone (1-4% reduction) due to the low amounts of bromine peaking up to about 1 ppt. *NO_x* levels were greatly reduced in the halogen emission case by the *ClO* reaction with *NO₂*, in some areas up to 50% compared to the run without halogens. Chlorine may therefore be a significant sink of *NO₂* in areas where the photodissociation of *ClONO₂* is slow.

Aknowledgement: The work reported here was funded by the EU Commission through the projects ARCTOC, HALOTROP-CYMFO and TACIA.

Number	Reaction (of order n)	n	$\frac{K^{\theta}}{M^{1-n} s^{-1}}$	Reference
G001	$O(^3P) + O_2 \rightarrow O_3$	2	$6.0 \times 10^{-34} (T/300)^{-2.8} O_2$ $5.6 \times 10^{-34} (T/300)^{-2.8} N_2$	Atkinson et al., 1997
G002	$O(^1D) + M \rightarrow O(^3P)$	2	$3.2 \times 10^{-11} O_2^{+70/T}$ $1.8 \times 10^{-11} N_2 \exp(110/T)$	DeMore, 1992
G003	$O(^3P) + NO \rightarrow NO_2$	2	$1.0 \times 10^{-31} (T/300)^{-1.6} N_2 (k_0)$ $3.0 \times 10^{-11} (T/300)^{0.3} (k_{\infty})$ $F_c = \exp(-T/1850)$	Atkinson et al., 1997
G004	$H_2O + O(^1D) \rightarrow 2OH$	2	2.2×10^{-10}	Atkinson et al., 1997
G005	$O_3 + NO \rightarrow NO_2$	2	$1.8 \times 10^{-12} \exp(-1370/T)$	Atkinson et al., 1997
G006	$O_3 + NO_2 \rightarrow NO_3$	2	$1.2 \times 10^{-13} \exp(-2450/T)$	Atkinson et al., 1997
G007	$O_3 + OH \rightarrow HO_2$	2	$1.9 \times 10^{-12} \exp(-1000/T)$	Atkinson et al., 1997
G008	$O_3 + HO_2 \rightarrow OH$	2	$1.4 \times 10^{-14} \exp(-600/T)$	Atkinson et al., 1997
G009	$NO + NO_3 \rightarrow 2NO_2$	2	$1.8 \times 10^{-11} \exp(110/T)$	Atkinson et al., 1997
G010	$NO + HO_2 \rightarrow NO_2 + OH$	2	$3.7 \times 10^{-12} \exp(240/T)$	Atkinson et al., 1997
G011	$NO_2 + NO_3 \rightarrow NO + NO_2$	2	$4.5 \times 10^{-14} \exp(-1260/T)$	Atkinson et al., 1997
G012	$NO_2 + NO_3 \rightarrow N_2O_5$	2	$2.7 \times 10^{-30} (T/300)^{-3.4} N_2 (k_0)$ $2.0 \times 10^{-12} (T/300)^{0.2} (k_{\infty})$ $F_c = \exp(-T/250)$	Atkinson et al., 1997
G013	$NO_2 + OH \rightarrow HNO_3$	2	$2.6 \times 10^{-30} (T/300)^{-2.5} N_2 (k_0)$ $6.7 \times 10^{-11} (T/300)^{-0.6} (k_{\infty})$ $F_c = 0.43$	Atkinson et al., 1997
G014	$NO_2 + HO_2 \rightarrow HO_2NO_2$	2	$1.8 \times 10^{-31} (T/300)^{-3.2} N_2 (k_0)$ $4.7 \times 10^{-12} (k_{\infty})$ $F_c = 0.6$	Atkinson et al., 1997
G015	$NO_3 + NO_3 \rightarrow 2NO_2$	2	2.7×10^{-16}	Wayne, 1991
G016	$NO_3 + H_2O_2 \rightarrow HO_2 + HNO_3$	2	2.0×10^{-15}	Wayne, 1991
G017	$N_2O_5 \rightarrow NO_2 + NO_3$	2	$1.0 \times 10^{-3} (T/300)^{-3.5}$ $\exp(-11000/T) N_2 (k_0)$ $9.7 \times 10^{14} (T/300)^{0.1}$ $\exp(-11080/T) (k_{\infty})$ $F_c = \exp(-T/250) \exp(-1050)$	Atkinson et al., 1997
G018	$N_2O_5 + H_2O \rightarrow 2HNO_3$	2	1.3×10^{-21}	EMEP
G019	$HO_2NO_2 \rightarrow NO_2 + HO_2$	1	$5.0 \times 10^{-6} \exp(-10000/T) N_2 (k_0)$ $2.6 \times 10^{15} \exp(-10900/T) (k_{\infty})$ $F_c = 0.6$	Atkinson et al., 1997
G020	$OH + H_2 \rightarrow HO_2$	2	$7.7 \times 10^{-12} \exp(-2100/T)$	Atkinson et al., 1997
G021	$OH + HO_2 \rightarrow$	2	$4.8 \times 10^{-11} \exp(250/T)$	Atkinson et al., 1997
G022	$OH + H_2O_2 \rightarrow HO_2$	2	$2.9 \times 10^{-12} \exp(160/T)$	Atkinson et al., 1997
G023	$OH + HO_2NO_2 \rightarrow NO_2$	2	$1.5 \times 10^{-12} \exp(360/T)$	Atkinson et al., 1997
G024	$HO_2 + HO_2 \rightarrow H_2O_2$	2	$2.3 \times 10^{-13} \exp(600/T) +$ $1.7 \times 10^{-33} \exp(1000/T) M \times$ $(1. + 1.4 \times 10^{-21} \exp(2200/T) H_2O)$	DeMore, 1992
G025	$OH + HNO_3 \rightarrow NO_3$	2	$7.2 \times 10^{-15} \exp(785/T) +$ $1.9 \times 10^{-33} \exp(725/T) M /$ $(1 + 1.9 \times 10^{-33} \exp(725/T) M /$ $4.1 \times 10^{-16} \exp(1440/T))$	Atkinson et al., 1997
G026	$CH_4 + OH \rightarrow CH_3O_2$	2	$2.3 \times 10^{-12} \exp(-1765/T)$	Atkinson et al., 1997
G027	$CH_4 + NO_3 \rightarrow CH_3O_2 + HNO_3$	2	4.0×10^{-19}	Atkinson et al., 1997
G028	$C_2H_6 + OH \rightarrow CH_3O_2$	2	$7.9 \times 10^{-12} \exp(1030/T)$	Atkinson et al., 1997
G029	$C_2H_6 + NO_3 \rightarrow CH_3O_2 + HNO_3$	2	1.0×10^{-12}	Singh and Zim., 1992
G030	$C_2H_4 + OH \rightarrow CH_3O_2$	2	2.0×10^{-17}	Mallard et al., 1993
G031	$C_2H_4 + O_3 \rightarrow HCHO + 0.42CO$ $+ 0.12HO_2 + 0.12H_2$	2	1.0×10^{-11} $9.1 \times 10^{-15} \exp(-2580/T)$	Singh and Zim., 1992
G032	$C_2H_4 + NO_3 \rightarrow CH_3O_2 + HNO_3$	2	$3.3 \times 10^{-12} \exp(-2880/T)$	Atkinson et al., 1997
G033	$C_2H_2 + OH \rightarrow HCOOH + CO + HO_2$	2	$5.0 \times 10^{-30} \exp(T/300)^{-1.5} N_2 (k_0)$ $9.0 \times 10^{-13} \exp(T/300)^{2.0} (k_{\infty})$ $F_c = 0.62$	Atkinson et al., 1997

Number	Reaction (of order n)	n	$\frac{K^0}{M^{1-n} - 1}$	Reference
G034	$CO + OH \rightarrow HO_2$	2	$1.3 \times 10^{-13} (1. + 0.6M)(300/T)$	Atkinson et al., 1997
G035	$CH_3O_2 + NO \rightarrow HCHO + HO_2 + NO_2$	2	$4.2 \times 10^{-12} \exp(180/T)$	Atkinson et al., 1997
G036	$CH_3O_2 + CH_3O_2 \rightarrow 2HCHO + 2HO_2$	2	$1.1 \times 10^{-13} \exp(365/T)$	Atkinson et al., 1997
G037	$CH_3O_2 + CH_3O_2 \rightarrow CH_3OH + HCHO$	2	$1.1 \times 10^{-13} \exp(365/T)$	Atkinson et al., 1997
G038	$CH_3OH + OH \rightarrow HCHO + HO_2$	2	$3.1 \times 10^{12} \exp(360/T)$	Atkinson et al., 1997
G039	$CH_3OH + NO_3 \rightarrow HCHO + HNO_3 + HO_2$	2	$1.3 \times 10^{-12} \exp(-2560/T)$	Atkinson et al., 1997
G040	$CH_3O_2 + HO_2 \rightarrow CH_3O_2H$	2	$3.8 \times 10^{-13} \exp(780/T)$	Atkinson et al., 1997
G041	$CH_3O_2H + OH \rightarrow HCHO + OH$	2	$1.0 \times 10^{-12} \exp(190/T)$	Atkinson et al., 1997
G042	$CH_3O_2H + OH \rightarrow CH_3O_2$	2	$1.9 \times 10^{-12} \exp(190/T)$	Atkinson et al., 1997
G043	$HCHO + OH \rightarrow CO$	2	$8.6 \times 10^{-12} \exp(20/T)$	Atkinson et al., 1997
G044	$HCHO + NO_3 \rightarrow CO + HO_2 + HNO_3$	2	5.8×10^{-16}	Atkinson et al., 1997
G045	$HCOOH + OH \rightarrow HO_2$	2	4.5×10^{-13}	Atkinson et al., 1997
G050	$HCl + OH \rightarrow H_2O + Cl$	2	$2.4 \times 10^{-12} \exp(-330/T)$	Atkinson et al., 1997
G051	$Cl + HO_2 \rightarrow HCl + O_2$	2	$1.8 \times 10^{-11} \exp(170/T)$	Atkinson et al., 1997
G052	$Cl + HO_2 \rightarrow ClO + OH$	2	$4.1 \times 10^{-11} \exp(-450/T)$	Atkinson et al., 1997
G053	$Cl + O_3 \rightarrow ClO + O_2$	2	$2.9 \times 10^{-11} \exp(-260/T)$	Atkinson et al., 1997
G054	$Cl + H_2O_2 \rightarrow HCl + O_2$	2	$1.1 \times 10^{-11} \exp(-980/T)$	Atkinson et al., 1997
G055	$Cl + NO_3 \rightarrow ClO + NO_2$	2	2.4×10^{-11}	Atkinson et al., 1997
G056	$Cl + CH_4 \rightarrow HCl + CH_3O_2$	2	$9.6 \times 10^{-12} \exp(-1350/T)$	Atkinson et al., 1997
G057	$Cl + C_2H_6 \rightarrow HCl + CH_3O_2$	2	$8.1 \times 10^{-11} \exp(-95/T)$	Atkinson et al., 1997
G058	$Cl + C_2H_4 \rightarrow HCl + CH_3O_2$	2	$1.6 \times 10^{-29} ((T/300)^{-3.5})M (k_0)$ $3.0 \times 10^{-10} (k_\infty)$ $F_c = 0.6$	Atkinson et al., 1997
G059	$Cl + C_2H_2 \rightarrow HCl$	2	$5.7 \times 10^{-30} ((T/300) - 3)N_2 (k_0)$ $2.3 \times 10^{-10} (k_\infty)$ $F_c = 0.6$	Atkinson et al., 1997
G060	$Cl + C_2H_2 \rightarrow 2CO + 2HO_2 + Cl$	2	$5.7 \times 10^{-30} ((T/300)^{-3})N_2$	Atkinson et al., 1997
G061	$Cl + C_2H_2 \rightarrow 2CO + 2HO_2 + Cl$	2	$5.7 \times 10^{-30} ((T/300)^{-3})N_2$	Atkinson et al., 1997
G062	$Cl + C_2H_2 \rightarrow 2CO + HO_2 + HCl$	2	$5.7 \times 10^{-30} ((T/300)^{-3})N_2$	Atkinson et al., 1997
G063	$Cl + CH_3OH \rightarrow HCl + HCHO + HO_2$	2	5.5×10^{-11}	Atkinson et al., 1997
G064	$Cl + CH_3O_2 \rightarrow ClO + HCHO + HO_2$	2	1.0×10^{-11}	Assumed
G065	$Cl + CH_3O_2 \rightarrow HCl + CO + H_2O$	2	5.0×10^{-12}	Assumed
G066	$Cl + HCHO \rightarrow HCl + HO_2 + CO$	2	$8.2 \times 10^{-11} \exp(-34/T)$	Atkinson et al., 1997
G067	$Cl + Cl_2O_2 \rightarrow Cl_2 + Cl + O_2$	2	1.0×10^{-10}	Atkinson et al., 1997
G068	$Cl_2 + OH \rightarrow HOCl + Cl$	2	$1.4 \times 10^{-12} \exp(-900/T)$	Atkinson et al., 1997
G069	$ClO + OH \rightarrow HO_2 + Cl$	2	$1.1 \times 10^{-11} \exp(120/T)$	Atkinson et al., 1997
G070	$ClO + OH \rightarrow HCl + O_2$	2	$1.1 \times 10^{-11} \exp(120/T)$	Atkinson et al., 1997
G071	$ClO + HO_2 \rightarrow HOCl + O_2$	2	$4.6 \times 10^{-13} \exp(710/T)$	Atkinson et al., 1997
G072	$ClO + O_3 \rightarrow Cl + 2O_2$	2	1.5×10^{-17}	Atkinson et al., 1997
G073	$ClO + O_3 \rightarrow O(^3P) + ClO + O_2$	2	1.0×10^{-18}	Atkinson et al., 1997
G074	$ClO + NO \rightarrow Cl + NO_2$	2	$6.2 \times 10^{-12} \exp(294/T)$	Atkinson et al., 1997
G075	$ClO + NO_2 \rightarrow ClONO_2$	2	$1.6 \times 10^{-31} (T/300)^{-3.4} N_2 (k_0)$ $2.0 \times 10^{-11} (k_\infty)$ $F_c = \exp(-T/430)$	Atkinson et al., 1997
G076	$ClO + NO_3 \rightarrow Cl + NO_2 + O_2$	2	4.7×10^{-13}	Atkinson et al., 1997
G077	$ClO + NO_3 \rightarrow O(^3P) + ClO + NO_2$	2	4.7×10^{-13}	Atkinson et al., 1997
G078	$ClO + CH_3O_2 \rightarrow Cl + HCHO + HO_2$	2	$4.9 \times 10^{-12} \exp(-330/T)$	Atkinson et al., 1997
G079	$ClO + ClO \rightarrow Cl_2O_2$	2	$1.7 \times 10^{-32} ((T/300)^{-4})N_2 (k_0)$ $5.4 \times 10^{-12} (k_\infty)$ $F_c = 0.6$	Atkinson et al., 1997
G080	$ClO + ClO \rightarrow Cl_2 + O_2$	2	$1.0 \times 10^{-12} \exp(-1590/T)$	Atkinson et al., 1997
G081	$ClO + ClO \rightarrow 2Cl + O_2$	2	$3.0 \times 10^{-11} \exp(-1590/T)$	Atkinson et al., 1997
G082	$ClO + ClO \rightarrow Cl + O(^3P) + ClO$	2	$3.5 \times 10^{-13} \exp(-1370/T)$	Atkinson et al., 1997
G083	$HOCl + OH \rightarrow ClO + H_2O$	2	$3.0 \times 10^{-12} \exp(-500/T)$	Atkinson et al., 1997
G084	$ClONO_2 + OH \rightarrow ClO + HNO_3$	2	$1.2 \times 10^{-12} \exp(-330/T)$	Atkinson et al., 1997
G085	$Cl_2O_2 \rightarrow ClO + ClO$	1	$1.0 \times 10^{-6} \exp(-8000/T)N_2 (k_0)$ $4.8 \times 10^{15} \exp(-8820/T)$	Atkinson et al., 1997

Number	Reaction (of order n)	n	$\frac{R^{\theta}}{M^{1-n} s^{-1}}$	Reference
G086	$Cl_2O_2 + O_3 \rightarrow ClO + Cl + 2O_2$	2	1.0×10^{-19}	Atkinson et al., 1997
G090	$HBr + OH \rightarrow Br + H_2O$	2	$1.1 \times 10^{-11} (T/298)^{-0.8}$	Atkinson et al., 1997
G091	$Br + O_3 \rightarrow BrO + O_2$	2	$1.7 \times 10^{-11} \exp(-800/T)$	Atkinson et al., 1997
G092	$Br + HO_2 \rightarrow HBr + O_2$	2	$1.4 \times 10^{-11} \exp(-590/T)$	Atkinson et al., 1997
G093	$Br + NO_3 \rightarrow BrO + NO_2$	2	1.6×10^{-11}	Atkinson et al., 1997
G094	$Br + C_2H_4 \rightarrow HBr + CH_3O_2$	2	1.6×10^{-13}	Bierbach et al., 1996
G095	$Br + C_2H_2 \rightarrow HBr + CO + HO_2$	2	$3.6 \times 10^{-14} \times 0.33$	Bierbach et al., 1996
G096	$Br + C_2H_2 \rightarrow Br + 2CO + 2HO_2$	2	$3.6 \times 10^{-14} \text{ times } 0.33$	Bierbach et al., 1996
G097	$Br + C_2H_2 \rightarrow HBr + 2CO + HO_2$	2	$3.6 \times 10^{-14} \text{ times } 0.33$	Bierbach et al., 1996
G098	$Br + CH_3OH \rightarrow HBr + HCHO + HO_2$	2	5.0×10^{-16}	Barnes, 1996
G099	$Br + CH_3O_2 \rightarrow BrO + CO$	2	5.0×10^{-14}	Assumed
G100	$Br + HCHO \rightarrow HBr + CO + HO_2$	2	$1.7 \times 10^{-11} \exp(-800/T)$	Atkinson et al., 1997
G101	$Br + Cl_2O_2 \rightarrow BrCl + Cl + O_2$	2	3.0×10^{-12}	Atkinson et al., 1997
G102	$Br + Cl_2 \rightarrow BrCl + Cl$	2	1.1×10^{-15}	Mallard et al., 1993
G103	$Br_2 + OH \rightarrow HOBr + Br$	2	$1.2 \times 10^{-11} \exp(400/T)$	Atkinson et al., 1997
G104	$Br_2 + Cl \rightarrow BrCl + Br$	2	1.2×10^{-10}	Mallard et al., 1993
G105	$BrCl + Br \rightarrow Br_2 + Cl$	2	3.3×10^{-15}	Mallard et al., 1993
G106	$BrCl + Cl \rightarrow Br + Cl_2$	2	1.5×10^{-11}	Mallard et al., 1993
G107	$BrO + HO_2 \rightarrow HOBr + O_2$	2	$6.2 \times 10^{-12} \exp(500/T)$	Atkinson et al., 1997
G108	$BrO + O_3 \rightarrow Br + 2O_2$	2	5.0×10^{-17}	Atkinson et al., 1997
G109	$BrO + NO \rightarrow Br + NO_2$	2	$8.7 \times 10^{-12} \exp(260/T)$	Atkinson et al., 1997
G110	$BrO + NO_2 \rightarrow BrONO_2$	2	$4.7 \times 10^{-31} (T/300)^{-3.1} N_2 (k_0)$ $1.7 \times 10^{-11} (T/300)^{-0.6} N_2 (k_{\infty})$ $F_c = \exp(-T/327)$	Atkinson et al., 1997
G111	$BrO + NO_3 \rightarrow Br + O_2 + NO_2$	2	1.0×10^{-12}	Atkinson et al., 1997
G112	$BrO + CH_3O_2 \rightarrow Br + HCHO + HO_2$	2	5.7×10^{-12}	LeBras, 1997
G113	$BrO + ClO \rightarrow Br + O(^3P) + ClO$	2	$1.6 \times 10^{-12} \exp(430/T)$	Atkinson et al., 1997
G114	$BrO + ClO \rightarrow Br + Cl + O_2$	2	$2.9 \times 10^{-12} \exp(220/T)$	Atkinson et al., 1997
G115	$BrO + ClO \rightarrow BrCl + O_2$	2	$5.8 \times 10^{-13} \exp(170/T)$	Atkinson et al., 1997
G116	$BrO + BrO \rightarrow 2Br + O_2$	2	$4.0 \times 10^{-12} \exp(-190/T)$	Atkinson et al., 1997
G117	$BrO + BrO \rightarrow Br_2 + O_2$	2	$4.2 \times 10^{-14} \exp(660/T)$	Atkinson et al., 1997

Table 3: Gas phase reactions included in the model.

Number	Reaction	$\frac{J}{s^{-1}}$	Reference
J01	$O_3 \rightarrow O(^1D)$	3.1×10^{-5}	DeMore et al., 1992
J02	$O_3 \rightarrow O(^3P)$	5.0×10^{-4}	DeMore et al., 1992
J03	$H_2O_2 \rightarrow 2.OH$	7.4×10^{-6}	DeMore et al., 1992
J04	$NO_2 \rightarrow O(^3P) + NO$	8.9×10^{-3}	DeMore et al., 1992
J05	$NO_3 \rightarrow NO$	2.6×10^{-2}	DeMore et al., 1992
J06	$NO_3 \rightarrow NO_2 + O(^3P)$	2.0×10^{-1}	DeMore et al., 1992
J07	$N_2O_5 \rightarrow NO_2 + NO_3$	4.5×10^{-5}	DeMore et al., 1992
J08	$HNO_3 \rightarrow NO_2 + OH$	6.0×10^{-7}	DeMore et al., 1992
J09	$HO_2NO_2 \rightarrow HO_2 + NO_2$	2.7×10^{-6}	DeMore et al., 1992
J10	$CH_3O_2H \rightarrow HCHO + OH + HO_2$	5.1×10^{-6}	DeMore et al., 1992
J11	$HCHO \rightarrow CO + 2.HO_2$	2.9×10^{-5}	DeMore et al., 1992
J12	$HCHO \rightarrow CO + H_2$	4.6×10^{-5}	DeMore et al., 1992
J20	$HOCl \rightarrow Cl + OH$	2.4×10^{-4}	Atkinson et al., 1997
J21	$Cl_2O_2 \rightarrow 2Cl + O_2$	1.3×10^{-3}	Atkinson et al., 1997
J22	$ClONO_2 \rightarrow Cl + NO_3$	5.0×10^{-5}	Atkinson et al., 1997
J23	$Cl_2 \rightarrow 2Cl$	2.4×10^{-3}	Atkinson et al., 1997
J30	$HOBr \rightarrow Br + OH$	2.0×10^{-3}	Rattigan et al., 1996
J31	$BrONO_2 \rightarrow Br + NO_3$	1.0×10^{-3}	Atkinson et al., 1997
J32	$Br_2 \rightarrow 2Br$	3.4×10^{-2}	Atkinson et al., 1997
J33	$BrCl \rightarrow Br + Cl$	1.1×10^{-2}	Atkinson et al., 1997
J34	$BrO \rightarrow Br + O(P)$	3.8×10^{-2}	Atkinson et al., 1997

Table 4: Photolysis rates in the gas phase. (Noon, no cloud values at 45°N, ozone column of 350 DU).

Species	Sea	land
O_3	0.02	0.5
H_2O_2	0.2	0.5
HO_2	0.2	0.2
NO_2	0.2	0.6
NO_3	0.1	0.5
N_2O_5	0.1	0.5
HNO_3	0.5	2.0
CH_3O_2H	0.5	0.5
CH_3O_2	0.2	0.2
$HCHO$	0.2	0.5
HCl	0.5	1.0
$HOCl$	0.2	0.2
HBr	0.5	1.0
$HOBr$	0.2	0.2
SO_2	0.4	0.8

Table 5: Dry deposition velocities (cm/s) over sea and land.

Specie	λ
HNO_3	1.4×10^6
SO_2	5.0×10^5
H_2O_2	5.0×10^5
CH_3O_2H	5.0×10^5
HCl	1.4×10^6
HBr	1.4×10^6

Table 6: Wet scavenging coefficients applied in the simulation.

References

- Anderson G.P., Clough S.A., Kneizys F.X., Chetwynd J.H. and Shettle E.P. (1986) AFGL Atmospheric Constituent profiles (0-120 km). *AFGL-TR-860110, AFGL (OPI), Hanscom AFB, MA 01736*.
- Barnes I., Bastian V., Becker R.H. and Overath R.D. (1991) Kinetic studies of the reactions of *IO*, *BrO* and *ClO* with *DMS*. *Int. J. Chem. Kin.*, Vol. 23, pp. 579-591.
- Barrie L.A., Bottenheim J.W., Schnell R.C., Crutzen P.J. and Rasmussen R.A. (1988) Ozone destruction and photochemical reactions at polar sunrise in the lower Arctic atmosphere. *Nature* 334, pp. 138-141.
- Beine H.J., Jaffe D.A., Stordal F., Engardt M., Solberg S., Schmidbauer N. and Holmen K. (1997) *NO_x* during ozone depletion events in the Arctic troposphere at Ny Ålesund, Svalbard. *Tellus*, Vol 49B, pp. 556-565.
- Bott A. (1989) A positive definite advection scheme obtained by nonlinear renormalization and fluxes. *Mon. Wea. Rev.*, 117 1006-1015.
- Bottenheim J., Barrie L., Atlas E., Heidt L. E., Niki H., Rasmussen R. A. and Shepson P. B. (1990) Depletion of lower tropospheric ozone during Arctic spring: The Polar Sunrise experiment 1988. *J. Geophys. Res.*, Vol 95, pp. 18555-18568.
- Burkholder J.B., Ravishankara A.R. and Solomon S. (1995) UV/visible and IR absorption cross sections for *BrONO₂*. *J. of Geophys. Res.*, Vol 100, pp. 16793-16800.
- Businger J.A., Wyngaard J.C., Izumi Y. and Bradley E.F. (1971) Flux profile relationships in the atmospheric surface layer. *J. Atm. Sci.*, Vol. 28, pp. 181-185.
- Chang J. S., Brost R. A., Isaksen I. S. A., Madronich S., Middleton P., Stockwell W. R. and Walcek C. J. (1987) A three-dimensional Eulerian acid deposition model: Physical concepts and formulation. *J. Geophys. Res.*, 92, D12, 14681-14700.
- de Serves C. (1994) Gas phase formaldehyde and peroxide measurements in the Arctic atmosphere. *J. of Geophys. Res.*, Vol. 99, pp. 25391-25398.
- Flatøy F. (1994) Modeling of coupled physical and chemical processes in the troposphere over Europe. *Dr. Scient dissertation, Geophysical. Inst., Univ. of Bergen, N-5007 Bergen, Norway*.
- Flatøy F. (1992) Comparison of two parameterization schemes for cloud and precipitation processes. *Tellus* 44A, 41-53.
- Fuchs N.A. and Sutugin A.G. (1971) High dispersed aerosols. *Topics in the current aerosol research. Ed. Hidy and Brock, pp. 1-60, Pergamon Press, New York*.
- Garcia R. and Solomon S. (1994) A new numerical model of the middle atmosphere: 2 - Ozone and related species. *J. of Geophys. Res.*, Vol 99, pp. 12937-12951.
- Grønås S., Foss A. and Lystad M. (1987) Numerical simulations of polar lows in the Norwegian Sea. *Tellus* 39A, 224-253.
- Hass H. (1991) Description of the EURAD Chemistry-Transport-Model Version 2 (CTM2). *Mitteilungen aus dem Institut für Geophysik und Meteorologie der Universität zu Köln, Heft 83*.
- Hausmann M. and Platt U. (1994) Spectroscopic measurements of bromine oxide and

ozone in the high Arctic during Polar Sunrise Experiment 1992. *J. Geophys. Res.*, Vol. 99, pp. 25,399-25,414.

Jobson B. T., Niki H., Yokouchi H., Bottenheim J., Hopper F. and Leitch R. (1994) Measurements of $C_2 - C_6$ hydrocarbons during the polar sunrise 92 experiment. Evidence for Cl-atom and Br-atom chemistry. *J. Geophys. Res.*, Vol 99, pp. 25355-25368.

Kvamstø N. G. (1992) Implementation of the Sundqvist scheme in the Norwegian Limited Area Model. *Meteorological report series, 2-92, Dep. of Geophys., Univ. of Bergen. 5007 Bergen, Norway.*

Kylling A., Stamnes K., Tsay S.C. (1995) A reliable and efficient 2-stream algorithm for spherical radiative transfer - Documentation of accuracy in realistic layered media. *J. of Atmospheric Chemistry*, Vol. 21, No 2 pp. 115-150.

Lary D.J. (1996) Gas phase atmospheric bromine photochemistry. *J. of Geophys. Res.*, Vol 101, pp. 1505-1516

Lary D.J., Chipperfield M.P., Toumi R. and Lenton T. (1996) Heterogeneous atmospheric bromine chemistry. *J. of Geophys. Res.*, Vol 101, pp. 1517.

Li S.M., Yokouchi Y., Barrie L.A., Muthuramu K., Shepson P.B., Bottenheim J.W., Sturges W.T. and Landsberger S. (1994) Organic and inorganic bromine compounds and their compositions in the Arctic troposphere during polar sunrise. *J. Geophys. Res.*, Vol. 99

Lugg G.A. (1968) Diffusion coefficients of some organic and other vapors in air. *Anal. Chem.*, 40, pp 1072-1077.

Marrero T.R. and Mason E.A. (1972) Gaseous diffusion coefficients. *J. Chem. Ref. Data*, 1 pp. 3-118.

McDonnell J.C., Henderson G.S., Barrie L., Bottenheim J., Niki H., Langford C.H. and Templeton E.M.J. (1992) Photochemical bromine production implicated in Arctic boundary layer ozone depletion. *Nature*, Vol. 355, pp. 150-152.

McKeen S. A., Hsie E.-Y., Trainer M., Tallamraju R. and Liu S. C. (1991) A regional model study of the ozone budget in the eastern United States. *J. Geophys. Res.*, 96, 10809-10845.

Mellouki A., Talukdar R.K. and Howard C.J. (1994) Kinetics of the reaction of HBr with ozone and HO_2 : The yield of HBr from $HO_2 + BrO$. *J. of Geophys. Res.*, Vol 99, pp. 22949-22954.

Minschwaner K., Salawitch R.J. and McElroy M.B. (1993) Absorption of solar radiation by O_2 : Implications for O_3 and lifetimes of N_2O , $CFCl_3$ and CF_2Cl_2 . *J. Geophys. Res.*, Vol 98, pp. 10543-10561.

Morris E. D. and Niki H. (1973) Reaction of dinitrogen pentoxide with water. *J. Phys. Chem.*, 77 1992 -2002

Mozourkewich M. (1995) Mechanisms for release of halogens from sea-salt particles by free radical reactions. *J. of Geophys. Res.*, Vol. 100, pp. 14199-14207.

Nordeng T. E. (1986) Parameterization of physical processes in a three-dimensional numerical weather prediction model. *Technical Report No. 65, DNMI, Oslo, Norway.*

Perner D., Trautmann A. and Zauner H. (1996) Measurements of atmospheric halogens

by neutron activation. *Arctic Tropospheric Ozone Chemistry (ARCTOC): Final report*, Ed. Platt U. and Lehrer E. Commission of European Communities, Brussels.

Platt U. (1998) HALOTROP-CYMFO Final report to the European Commission. *In preparation*

Pleim J. E. and Chang J. S. (1992) A non-local closure model for vertical mixing in the convective boundary layer. *Atmospheric Environment*, 26, 965-981.

Poulet G., Pirre M., Maguin F., Ramaroson R. and LeBras G. (1992) The role of the $HO_2 + BrO$ reaction in the stratospheric chemistry of bromine. *Geophys. Res. Lett.*, Vol. 19, pp. 2305-2308.

Ramacher B., Rudolph J. and Koppmann R. (1997) Hydrocarbon measurements in the spring Arctic troposphere during the ARTOC 95 campaign. *Tellus*, Vol 49B, pp. 446-485.

Sander R. and Crutzen P.J. (1996) Model study indicating halogen activation and ozone destruction in polluted air masses transported to the sea. *J. of Geophys. Res.*, Vol. 101, pp. 9121-9138.

Schall C., Laturus F. and Heumann K.G. (1994) Biogenic volatile organoiodine and organobromine compounds released from polar macroalgae. *Chemosphere*, Vol. 28, pp. 1315-1324.

Schwartz S.E. (1986) Mass transport considerations pertinent to aqueous phase reactions of gases in liquid water clouds. *Chemistry of multiphase systems, NATO ASI Ser.*, Vol G6, Ed. W Jaeschke, pp. 415-471, Springer Verlag, New York.

Sherwood T.K., Pigford R.L. and Wilke C.R. (1975) *Mass transfer*. McGraw-Hill, New York.

Solberg S., Schmidbauer N., Semb A., Stordal F. (1996) Boundary layer ozone depletion as seen in the Norwegian Arctic Spring. *J. Atm. Chem.*, Vol 23, pp. 301-332.

Strand A. and Hov Ø. (1993) A two dimensional zonally averaged transport model including convective motions and a new strategy for the numerical solution. *J. Geophys. Res.*, 98, 9023-9037.

Sturges W.T. and Harrison R.M. (1986) Bromine in marine aerosols and the origin, nature and quantity of natural atmospheric bromine. *Atmos. Environ.*, Vol 20, pp. 1485-1496.

Sundqvist H., Berge E. and Kristjanson J. E. (1989) Condensation and cloud parameterization studies with a mesoscale NWP model. *Mon. Wea. Rev.*, 117, 1641-1657.

Sundqvist H. (1988) Parameterization of condensation and associated clouds in models for weather prediction and general circulation simulations. *Physical based modelling and simulation of climate and climatic change* (ed. M. E. Schlesinger), Reidel, Dordrecht, 433-461.

Toumi R. (1994) BrO as a sink for dimethylsulphide in marine atmosphere. *Geophys. Res. Lett.*, Vol. 21, pp 117-120.

Tuckermann M., Ackermann R., Golz C., Lorenzen-Schmidt, H., Senne T., Stultz J., Trost B., Unold W. and Platt U. (1997) DOAS observation of halogen radical-catalysed Arctic boundary layer ozone destruction during the ARCTOC campaigns 1995 and 1996 in Ny Ålesund, Spitsbergen. *Tellus*, Vol 49B, pp. 533-555.

Vogt R., Crutzen P. J. and Sander R. (1996) A mechanism for halogen release from

sea-salt aerosol in the remote marine boundary layer. *Nature*, Vol 389, pp 327-330.